Results in Physics 20 (2021) 103669

Contents lists available at ScienceDirect

Results in Physics

journal homepage: www.elsevier.com/locate/rinp

Modeling and analysis of the dynamics of novel coronavirus (COVID-19) with Caputo fractional derivative

Aatif Ali [a], Fehaid Salem Alshammari [b], Saeed Islam [a], Muhammad Altaf Khan [c,d,*], Saif Ullah [e]

[a] Department of Mathematics, Abdul Wali Khan University Mardan, Khyber Pakhtunkhwa, Pakistan
[b] Department of Mathematics and Statistics, Imam Mohammad Ibn Saud, Islamic University, 13318 Riyadh, Saudi Arabia
[c] Informetrics Research Group, Ton Duc Thang University, Ho Chi Minh City, Viet Nam
[d] Faculty of Mathematics and Statistics, Ton Duc Thang University, Ho Chi Minh City, Viet Nam
[e] Department of Mathematics, University of Peshawar Khyber Pakhtunkhwa, Pakistan

ARTICLE INFO

Keywords:
Fractional Caputo derivative
COVID-19
Non-pharmaceutical intervention
Stability
Parameter estimation
Numerical simulations

ABSTRACT

The new emerged infectious disease that is known the coronavirus disease (COVID-19), which is a high contagious viral infection that started in December 2019 in China city Wuhan and spread very fast to the rest of the world. This infection caused million of infected cases globally and still pose an alarming situation for human lives. Pakistan in Asian countries is considered the third country with higher number of cases of coronavirus with more than 200,000. Recently, many mathematical models have been considered to better understand the coronavirus infection. Most of these models are based on classical integer-order derivative which can not capture the fading memory and crossover behavior found in many biological phenomena. Therefore, we study the coronavirus disease in this paper by exploring the dynamics of COVID-19 infection using the non-integer Caputo derivative. In the absence of vaccine or therapy, the role of non-pharmaceutical interventions (NPIs) is examined on the dynamics of theCOVID-19 outbreak in Pakistan. First, we construct the model in integer sense and then apply the fractional operator to have a generalized model. The generalized model is then used to present the detailed theoretical results. We investigate the stability of the model for the case of fractional model using a nonlinear fractional Lyapunov function of Goh-Voltera type. Furthermore, we estimate the values of parameters with the help of least square curve fitting tool for the COVID-19 data recorded in Pakistan since March 1 till June 30, 2020 and show that our considered model give an accurate prediction to the real COVID-19 statistical cases. Finally, numerical simulations are presented using estimated parameters for various values of the fractional order of the Caputo derivative. From the simulation results it is found that the fractional order provides more insights about the disease dynamics.

1. Introduction

A highly contagious viral disease caused by a coronavirus (SARS-CoV-2), first identified in China at the end of 2019 and affecting 213 countries and territories around the world [22]. The novel Wuhan virus figures under different names such as the novel coronavirus (2019-nCoV) on January 7 and COVID-19 by the World Health Organization (WHO) on February 11 [38]. The transmission of the virus was considered initially animal-to-human and fist human-to-human transmission confirmed on January 20 in Guangdong, a coastal province of southeast China [38,12]. Over 10.27 million confirmed cases and more than 0.5 million cumulative deaths all over the world are recorded till June 30, 2020 [1]. The mortality rate is about 7% and the recovery rate is 93% globally [1,22]. The pharmaceutical companies, regulatory authorities are doing every thing possible for the availability of a safe and effective anti-viral vaccine against this novel infection. The pandemic continuously inflects severe public health, hit the laborer's community and economy throughout the world, including in Pakistan. The suggested incubation period for this viral infection is in the range 2 to 10 days by WHO [25,12]. The symptoms of a COVID-19 infected person include fever, myalgia or fatigue, dry cough, shortness of breath or dyspnoea, pneumonia, chills, sore throat, multiple organ failure, anorexia or lungs failure, acute respiratory distress syndrome (ARDS), lymphopenia (a reduction of lymphocytes in the circulating blood), loss of smell or taste and a sign of cytokine storm [25,12]. The majority of deaths have occurred in other chronic illnesses like diabetes, hypertension and

* Corresponding author.
E-mail address: muhammad.altaf.khan@tdtu.edu.vn (M.A. Khan).

https://doi.org/10.1016/j.rinp.2020.103669
Received 21 September 2020; Received in revised form 25 November 2020; Accepted 27 November 2020
Available online 14 December 2020

cardiovascular disease. In the absence of therapies, approved vaccine and antiviral the whole world is focusing on non-pharmaceutical interventions to eradicate this COVID-19. The most common NPIs practices these days are social physical distance, exposed to be a quarantine, isolation of infected, wearing mask, more testing facility, closure of the school, non-essential business, hand washing or sanitizing, lockdown (stay at home and work from home) and protective kit for medical personal and avoiding unnecessary gathering.

Pakistan is one of the epicenters of COVID-19 in Asia with an estimated population of over 220 million [1]. Currently, Pakistan is the 3rd country in Asia and 12th in the world with high confirmed infected cases [17,1]. As on 30 June 2020, 209,337 total confirmed cases are recorded and about 4304 lost their lives. Although in Pakistan the mortality rate is very low as compared to the recovery rate, still this disease has a negative impact on the economy. The first case reported in Karachi on 26 Feb 2020, the virus spread quickly within three weeks in the entire country. Also, the accounted cases are less than the total cases due to limiting testing. Currently, the situation is worse, due to open lockdown on 9 May, the government is unable to maintain strict lockdown because of severe economic hardship. But the government imposed smart lockdown and easing restrictions, by allowing offices, business, markets with limited hours and staff capacity, five days in a week to reopen the economy of the country.

Mathematical models coupled with statistical data and its analysis are better to obtained reasonable information about the coronavirus disease and its complications and future spread and control. Recently, it is a huge challenge that without vaccines, how to curtail the pandemic with non-pharmaceutical intervention (NPIs). In this regard, different mathematical modeling approaches have been adopted to analyze the transmission pattern of COVID-19. Ferguson et al. [16] studied a COVID-19-induced mortality model with the impact of NPIs. A mathematical model for accessing the community-wide impact of mask in controlling the spread of coronavirus is developed by Eikenberry et al. [14]. The dynamics and mitigation strategies for COVID-19 in Canada have been studied in [39]. A compartmental system describing the coronavirus dynamics in three highly infected countries has been suggested in [15]. Recently, Ullah and Khan studied the coronavirus model for Pakistani data using optimal control theory [32]. Fractional calculus is the generalization of classical calculus. Mathematical models with non-integer order operators provide a better understanding of a phenomena. Further, models with fractional order derivatives are capable to capture the fading memory and crossover behavior and provides a greater degree of accuracy. Mathematical models with fractional derivative gives more insights about a disease under consideration [11,26,29,30]. Different fractional operators with singular and non-singular kernel were suggested in literature [5,27]. The applications of these fractional operators can be found in recent literature and references therein [3,8,9,20,33–35]. Recently, very few COVID-19 models based on fractional order operators are proposed. The dynamics of (2019-nCoV) fractional derivative to explore the situation of the pandemic in Wuhan is studied by Khan and Atangana [19]. Some other work about the mathematical models and its applications to fractional operators can be seen in [28,36,21,6,7,23,18].The authors in [28] considered a mathematical model for hepatitis C in fractional derivative and examined its results. The CoVID-19 model and its dynamical analysis using fuzzy Caputo differential equation is considered in [36]. The TB dynamics with relapse has been considered in [21] where the authors explored the results using conformable derivative. Some interesting results regarding fractional calculus and its connection to attract many physical structure is studied in [6]. The authors in [18] obtained the stability and numerical results for a HIV/AIDS model in fractional derivative. The oxygen diffusion problem in various fractional operators is discussed in [23]. A novel fractional-fractal operator with the singular and nonsingular kernel is applied to obtain a dynamical model for coronavirus is studied in [4]. Baleanu et al. [10] examined the dynamical investigations of coronaries model in fractional derivative using exponential kernel. A fractional order COVID-19 model in Caputo sense is recently studied in [31]. A more recent work on coronavirus considering the infected cases observed in Kingdom of Saudi Arabia is investigated in [2].

Motivated by the above discussion, currently in this work, we study the dynamical analysis of the COVID-19 model presented in [32], considering the Caputo operator in order to gain more insights about the pandemic. We consider here the real infected cases of novel coronavirus in Pakistan and obtain the results. A detailed theoretical analysis of the fractional order COVID-19 model is presented. Further, we estimate model parameters and the basic reproduction number using confirmed COVID-19 cases reported from the beginning of the outbreak till June 30, 2020 in Pakistan. The impact of important model parameters is shown for various values of the arbitrary fractional order of the Caputo operator. The rest of paper organization is as follows: The basics concepts related to fractional order derivatives are presented in Section 2. The model formulation in integer with parameter estimation and curve fitting to reported cases and its generalization to the fractional order derivative are presented in Section 3. Section 4 contains the analysis of the model and its stability results. In Section 5, we determine the important parameters and there impact on the basic reproduction number through sensitivity analysis is presented. The graphical results through biological discussion is depicted in Section 6. In Section 7, the work has been summarized with important suggestions about the disease control in the society.

2. Preliminaries on fractional derivative

In this section, we briefly discuss background material from fractional calculus.

Definition 1. Consider $u \in C^n$ be a function then the Caputo definition with α in $(r-1, r)$ where $r \in \mathbb{N}$ [27] is defined as:

$$ {}^{C}D_t^{\alpha}(u(t)) = \frac{1}{\Gamma(r-\alpha)} \int_0^t \frac{u^n(\varpi)(t-\varpi)^{r-\alpha}}{(t-\varpi)} d\varpi, $$

obviously, ${}^{C}D_t^{\alpha}(u(t))$ approaches to $u'(t)$ whenever $\alpha \to 1$.

Definition 2. The fractional integral having of order $\alpha > 0$ of the function $u : \mathbb{R}^+ \to \mathbb{R}$ is

$$ I_t^{\alpha}(u(t)) = \frac{1}{\Gamma(\alpha)} \int_0^t \frac{u(\varpi)(t-\varpi)^{\alpha}}{(t-\varpi)} d\varpi. $$

where $0 < \alpha < 1,\ t > 0$.

Definition 3. A generalized Mittag–Leffler function has been developed by Atangana and Baleanu defined as [5]:

$$ {}^{ABC}{}_{a}D_t^{\alpha}(u(t)) = \frac{ABC(\alpha)}{(1-\alpha)} \int_a^t u'(\varpi) E_{\alpha}\Big[-\alpha \frac{(t-\varpi)^{\alpha}}{1-\alpha}\Big] d\varpi, $$

where $\alpha \in [0, 1)$.

Definition 4. The associated fractional integral of the ABC derivative is defined as;

Table 1
Definitions of the variables of the system (1).

State variable	Definition
S	Susceptible people
E	Exposed people
I	Symptomatically-infectious people
I_a	Asymptomatically-infectious people
Q	Quarantined people
I_h	Hospitalized people
I_c	Critically infected people
R	Recovered people
N	Total population

Table 2
Estimated and fitted values along with description of the model parameters.

Symbol	Definition	Value/day	Ref
Λ	Requitement rate	$\mu^*N(0)$	Estimated
μ	Natural mortality rate	$\frac{1}{(365\times 67.7)}$	[1]
ξ_1	COVID-19 induced mortality rate in symptomatic class	0.022	[17]
ψ	Transmissibility rate relative to I_a class	0.5620	Fitted
ω	Incubation period	0.2691	Fitted
θ	Proportion of the symptomatic infection	0.2350	Fitted
γ	Rate at which symptomatic class are hospitalized	0.4507	Fitted
ξ_2	COVID-19 induced mortality rate in hospitalized class	0.0131	Fitted
ξ_3	COVID-19 induced death in critically-infected class	0.1622	Fitted
ϕ_1	Recovery or removal rate of quarantined class	0.4870	Fitted
ϕ_2	Recovery or removal rate of hospitalized class	0.5431	Fitted
ϕ_3	Recovery or removal rate of critically infected class	0.3838	Fitted
ϑ_1	Rate of recovery in I	0.6381	Fitted
ϑ_2	Rate of Rate of recovery in I_a	0.0803	Fitted
δ	Quarantined rate of exposed individuals	0.3716	Fitted
β	Infection transmission coefficient	0.7806	Fitted
ζ	Hospitalization rate of quarantined individuals	0.1396	Fitted
τ	Transmissibility of infection relative to I_h class	0.4826	Fitted
ϕ	Moving rate of I_H to I_c class	0.4593	Fitted

$$ {}^{ABC}_{a}I^{\alpha}_{t}(u(t)) = \frac{1-\alpha}{ABC(\alpha)}u(t) + \frac{\alpha}{ABC(\alpha)\Gamma(\alpha)}\int_a^t u(\varpi)(t-\varpi)^{\alpha-1}d\varpi, $$

where $\alpha \in [0,1)$.

Definition 5. [37] Consider a constant point for the Caputo system say y^* which is known to be its equilibrium point then,

$$ {}^{C}D^{\alpha}_{t}y(t) = u(t,y(t)), \quad \alpha \in (0,1), $$

if and only if $u(t,y^*) = 0$.

3. The classical integer order model

In this section, we briefly present description of the COVID-19 model in integer case. The model was recently proposed in [32]. To formulate the mathematical model, the whole population at time t, denoted by $N(t)$ is further split into eight mutually-exclusive sub-classes including susceptible $S(t)$, exposed $E(t)$, those infected people who infected after some specific incubation period with symptoms (or symptomatic infected) $I(t)$, those have no specific disease symptoms (or asymptotically infected individuals) $I_a(t)$, quarantined class $Q(t)$, individuals which are in hospitals or in self-isolation at home $I_h(t)$, critically-infected or COVID-19 infected people who were in ICU $I_c(t)$ and finally, the individuals successfully recovered from the infection is denoted by $R(t)$. In the class $I_a(t)$ infected individual showing mild or no symptoms and the class $I_h(t)$ contains the patient admitted into the hospital and those who are self-isolating at home with clinical symptoms. The state variables of the model are described in Table 1, while the complete description of the model parameters are describe in Table 2. The flow of among model compartments is depicted in Fig. 1. The COVID-19 transmission model rely on these subgroups and at the rate they interact, governed the non-linear system of ordinary differential equations as follows:

$$ \begin{cases} \frac{dS}{dt} = \Lambda - \frac{\beta(I+\psi I_a+\tau I_h)}{N}S - \mu S, \\ \frac{dE}{dt} = \frac{\beta(I+\psi I_a+\tau I_h)}{N}S - (\omega+\delta+\mu)E, \\ \frac{dI}{dt} = \theta\omega E - (\vartheta_1+\mu+\xi_1+\gamma)I, \\ \frac{dI_a}{dt} = (1-\theta)\omega E - (\vartheta_2+\mu)I_a, \\ \frac{dQ}{dt} = \delta E - (\mu+\phi_1+\zeta)Q, \\ \frac{dI_h}{dt} = \gamma I + \zeta Q - (\mu+\phi_2+\xi_2+\phi)I_h, \\ \frac{dI_c}{dt} = \phi I_h - (\mu+\phi_3+\xi_3)I_c, \\ \frac{dR}{dt} = \vartheta_1 I + \vartheta_2 I_a + \phi_1 Q + \phi_2 I_h + \phi_3 I_c - \mu R, \end{cases} \tag{1} $$

subjected to initial conditions

$$ S(0) = S_0, E(0) = E_0, I(0) = I_0, I_a(0) = I_{a0}, \\ Q(0) = Q_0, I_h(0) = I_{h0}, I_c(0) = I_{c0}, R(0) = R_0. $$

3.1. Parameter estimations

The purpose of this section is to estimate the parameters with help of the least square curve fitting from the confirmed cases of coronavirus that notified in Pakistan since March 1 till 30 June 2020. The recruitment as well as the natural death rate respectively given by Λ and μ are estimated from literature and the rest of the parameter values are fitted from the reported data. The detailed estimation procedure can be found in [32]. The best fitted model predicted curve is shown graphically in Fig. 2 and the model parameters with resulting estimated or fitted numerical values are shown in the Table 2. The numerical value of the $\mathscr{R}_0$ obtained via the fitted parameters is $\mathscr{R}_0 \approx 1.8870$, which is in agreement to the value estimated in recently published article [32].

3.2. Model in Caputo sense

In this subsection, we formulate the fractional order COVID-19 mathematical model. In order to observe the memory effects, the system (1), in term of integral as:

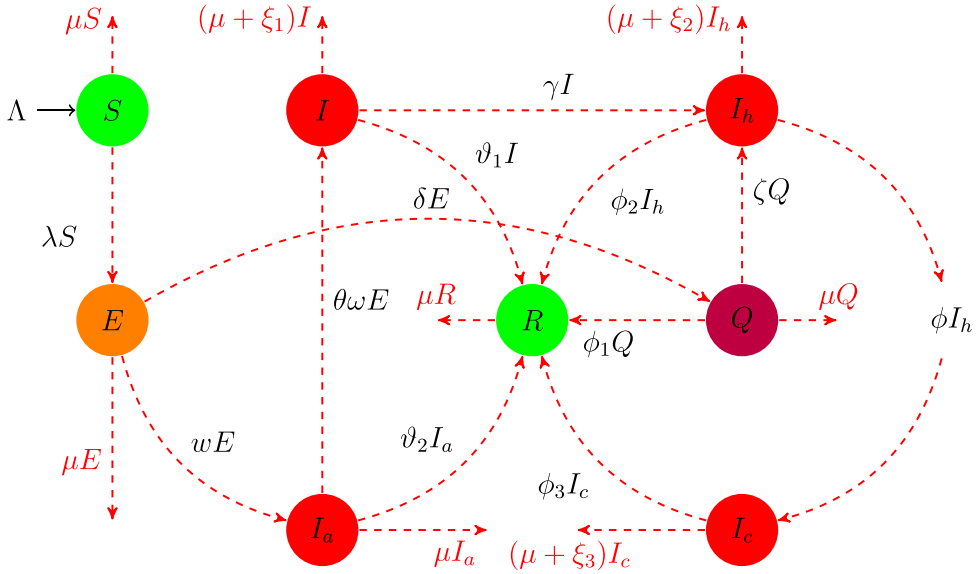

Fig. 1. Flow diagram of COVID-19 model.

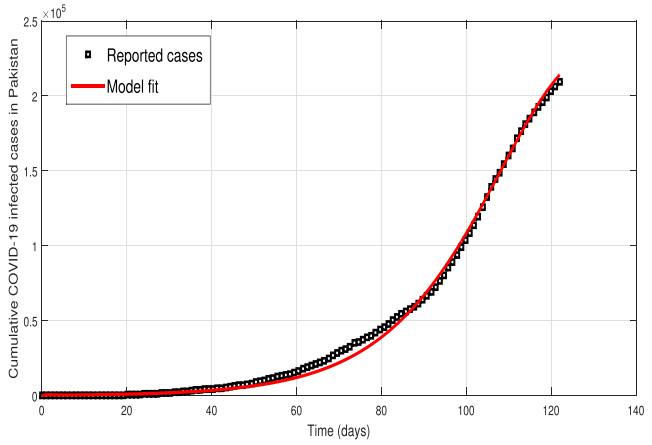

Fig. 2. Curve fitting (solid red line) to the confirmed infected cases using model (1). The data is consider from 1 March to 30 June 2020.

$$
\begin{cases}
\dfrac{dS}{dt} = \displaystyle\int_{t_0}^{t} k(t-t')\left[\Lambda - \frac{\beta(I+\psi I_a+\tau I_h)}{N}S - \mu S\right]dt', \\
\dfrac{dE}{dt} = \displaystyle\int_{t_0}^{t} k(t-t')\left[\frac{\beta(I+\psi I_a+\tau I_h)}{N}S - (\omega+\delta+\mu)E\right]dt', \\
\dfrac{dI}{dt} = \displaystyle\int_{t_0}^{t} k(t-t')[\theta\omega E - (\vartheta_1+\mu+\xi_1+\gamma)I]dt', \\
\dfrac{dI_a}{dt} = \displaystyle\int_{t_0}^{t} k(t-t')[(1-\theta)\omega E - (\vartheta_2+\mu)I_a]dt', \\
\dfrac{dQ}{dt} = \displaystyle\int_{t_0}^{t} k(t-t')[\delta E - (\mu+\phi_1+\zeta)Q]dt', \\
\dfrac{dI_h}{dt} = \displaystyle\int_{t_0}^{t} k(t-t')[\gamma I + \zeta Q - (\mu+\phi_2+\xi_2+\phi)I_h]dt', \\
\dfrac{dI_c}{dt} = \displaystyle\int_{t_0}^{t} k(t-t')[\phi I_h - (\mu+\phi_3+\xi_3)I_c]dt', \\
\dfrac{dR}{dt} = \displaystyle\int_{t_0}^{t} k(t-t')[\vartheta_1 I + \vartheta_2 I_a + \phi_1 Q + \phi_2 I_h + \phi_3 I_c - \mu R]dt',
\end{cases}
\tag{2}
$$

where, $k(t-t')$ act as time-dependent kernel and by power-law correlation function as:

$$
k(t-t') = \frac{1}{\Gamma(\alpha-1)}(t-t')^{\alpha-2}, \tag{3}
$$

Substituting the value of kernel in Eq. (2), and then applying the Caputo fractional derivative of order $\alpha-1$, then we have;

$$
\begin{cases}
{}^{C}D_t^{\alpha-1}\left[\dfrac{dS}{dt}\right] = {}^{C}D_t^{\alpha-1}I_t^{-(\alpha-1)}\left[\Lambda - \dfrac{\beta(I+\psi I_a+\tau I_h)}{N}S - \mu S\right], \\
{}^{C}D_t^{\alpha-1}\left[\dfrac{dE}{dt}\right] = {}^{C}D_t^{\alpha-1}I_t^{-(\alpha-1)}\left[\dfrac{\beta(I+\psi I_a+\tau I_h)}{N}S - (\omega+\delta+\mu)E\right], \\
{}^{C}D_t^{\alpha-1}\left[\dfrac{dI}{dt}\right] = {}^{C}D_t^{\alpha-1}I_t^{-(\alpha-1)}[\theta\omega E - (\vartheta_1+\mu+\xi_1+\gamma)I], \\
{}^{C}D_t^{\alpha-1}\left[\dfrac{dI_a}{dt}\right] = {}^{C}D_t^{\alpha-1}I_t^{-(\alpha-1)}[(1-\theta)\omega E - (\vartheta_2+\mu)I_a], \\
{}^{C}D_t^{\alpha-1}\left[\dfrac{dQ}{dt}\right] = {}^{C}D_t^{\alpha-1}I_t^{-(\alpha-1)}[\delta E - (\mu+\phi_1+\zeta)Q], \\
{}^{C}D_t^{\alpha-1}\left[\dfrac{dI_h}{dt}\right] = {}^{C}D_t^{\alpha-1}I_t^{-(\alpha-1)}[\gamma I + \zeta Q - (\mu+\phi_2+\xi_2+\phi)I_h], \\
{}^{C}D_t^{\alpha-1}\left[\dfrac{dI_c}{dt}\right] = {}^{C}D_t^{\alpha-1}I_t^{-(\alpha-1)}[\phi I_h - (\mu+\phi_3+\xi_3)I_c], \\
{}^{C}D_t^{\alpha-1}\left[\dfrac{dR}{dt}\right] = {}^{C}D_t^{\alpha-1}I_t^{-(\alpha-1)}[\vartheta_1 I + \vartheta_2 I_a + \phi_1 Q + \phi_2 I_h + \phi_3 I_c - \mu R],
\end{cases}
\tag{4}
$$

Both are the inverse operators then we will get the system (4),

$$\begin{cases} {}^{C}D_t^{\alpha}S(t) = \Lambda - \dfrac{\beta(I+\psi I_a+\tau I_h)}{N}S - \mu S, \\ {}^{C}D_t^{\alpha}E(t) = \dfrac{\beta(I+\psi I_a+\tau I_h)}{N}S - (\omega+\delta+\mu)E, \\ {}^{C}D_t^{\alpha}I(t) = \theta\omega E - (\vartheta_1+\mu+\xi_1+\gamma)I, \\ {}^{C}D_t^{\alpha}I_a(t) = (1-\theta)\omega E - (\vartheta_2+\mu)I_a, \\ {}^{C}D_t^{\alpha}Q(t) = \delta E - (\mu+\phi_1+\zeta)Q, \\ {}^{C}D_t^{\alpha}I_h(t) = \gamma I + \zeta Q - (\mu+\phi_2+\xi_2+\phi)I_h, \\ {}^{C}D_t^{\alpha}I_c(t) = \phi I_h - (\mu+\phi_3+\xi_3)I_c, \\ {}^{C}D_t^{\alpha}R(t) = \vartheta_1 I + \vartheta_2 I_a + \phi_1 Q + \phi_2 I_h + \phi_3 I_c - \mu R. \end{cases} \tag{5}$$

Let

$$\lambda(t) = \frac{\beta(I+\psi I_a+\tau I_h)}{N},$$

and

$$K_1 = (\omega+\delta+\mu), K_2 = (\vartheta_1+\mu+\xi_1+\gamma),\ K_3 = (\vartheta_2+\mu),$$
$$K_4 = (\mu+\phi_1+\zeta), K_5 = (\mu+\phi_2+\xi_2+\phi), K_6 = (\mu+\phi_3+\xi_3).$$

Then the novel coronavirus COVID-19 model in Caputo derivative form is;

$$\begin{cases} {}^{C}D_t^{\alpha}S(t) = \Lambda - \lambda S - \mu S, \\ {}^{C}D_t^{\alpha}E(t) = \lambda S - K_1 E, \\ {}^{C}D_t^{\alpha}I(t) = \theta\omega E - K_2 I, \\ {}^{C}D_t^{\alpha}I_a(t) = (1-\theta)\omega E - K_3 I_a, \\ {}^{C}D_t^{\alpha}Q(t) = \delta E - K_4 Q, \\ {}^{C}D_t^{\alpha}I_h(t) = \gamma I + \zeta Q - K_5 I_h, \\ {}^{C}D_t^{\alpha}I_c(t) = \phi I_h - K_6 I_c, \\ {}^{C}D_t^{\alpha}R(t) = \vartheta_1 I + \vartheta_2 I_a + \phi_1 Q + \phi_2 I_h + \phi_3 I_c - \mu R, \end{cases} \tag{6}$$

subjected to the non-negative initial conditions.

$$S(0)\geqslant 0, E(0)\geqslant 0, I(0)\geqslant 0, I_a(0)\geqslant 0, Q(0)\geqslant 0, I_h(0)\geqslant 0, I_c(0)\geqslant 0, R(0)\geqslant 0. \tag{7}$$

In the above Caputo system (6), the model developed here has eight components, $S, V, E, I, I_a, Q, I_h, I_c$ and R known as COVID-19 model of disease transmission also called fractional differential equations (FDEs) of eight-dimensional dynamical system.

3.3. Properties of the model

We provide in details in the following the model important properties.

3.4. Invariant region and attractivity

The dynamics of the fractional model (6) will be analyzed in the following biologically-feasible region,

$$\Xi \subset \mathbb{R}_+^8,$$

such thats

$$\Xi = \Big\{ \big(S(t),E(t),I(t),I_a(t),Q(t),I_h(t),I_c(t),R(t)\big) \in \mathbb{R}_+^8 : S(t)+E(t)+I(t)+I_a(t) + Q(t)+I_h(t)+I_c(t)+R(t) \leqslant \frac{\Lambda}{\mu} \Big\}.$$

Lemma 3.1. *The region given by $\Xi \subset \mathbb{R}_+^8$, is positively invariant for the system (6) with the initial conditions in $\mathbb{R}_+^8$.*

Proof. We have the following for the model (6),

$${}^{C}D_t^{\alpha}N(t) = {}^{C}D_t^{\alpha}S(t) + {}^{C}D_t^{\alpha}E(t) + {}^{C}D_t^{\alpha}I(t) + {}^{C}D_t^{\alpha}I_a(t) + {}^{C}D_t^{\alpha}Q(t) + {}^{C}D_t^{\alpha}I_h(t) + {}^{C}D_t^{\alpha}I_c(t) + {}^{C}D_t^{\alpha}R(t).$$

Hence,

$${}^{C}D_t^{\alpha}N(t) = \Lambda - \mu N(t) - \xi_1 I(t) - \xi_2 I_h(t) - \xi_3 I_c(t) \leqslant \Lambda - \mu N(t),$$

clearly we have,

$${}^{C}D_t^{\alpha}N(t) + \mu N(t) \leqslant \Lambda.$$

By applying the Laplace transform,

$$L[{}^{C}D_t^{\alpha}N(t) + \mu N(t)] \leqslant L[\Lambda],$$

$$s^{\alpha}N(s) - s^{\alpha-1}N(0) + \mu N(s) \leqslant \frac{\Lambda}{s},$$

$$N(s) \leqslant \frac{\Lambda}{s(s^{\alpha}+\mu)} + N(0)\frac{s^{\alpha-1}}{s^{\alpha}+\mu}.$$

Applying Laplace inverse, we obtain,

$$N(t) \leqslant N(0)E_{\alpha,1}(-\mu t^{\alpha}) + \Lambda t^{\alpha}E_{\alpha,\alpha+1}(-\mu t^{\alpha}),$$

The Mittag–Leffler function describe by infinite power series i.e;

$$E_{\alpha,\beta(z)} = \sum_{k=0}^{\infty} \frac{z^k}{\Gamma(\alpha k+\beta)},$$

and laplace transform of Mittag–leffler function is

$$L[t^{\beta-1}E_{\alpha,\beta}(\pm\alpha t^{\alpha})] = \frac{s^{\alpha-\beta}}{s^{\alpha} \mp \alpha}.$$

So $N(t)$ converges for $t \to \infty$ and for all $t > 0$ the solutions of the model with initial conditions in Ξ remain in Ξ. Thus, the region Ξ is positively invariant and attracts all solutions in $\mathbb{R}_+^8$. To show that the model has positive solution, we consider

$$\mathbb{R}_+^8 = \{y \in \mathbb{R}^8 | y \geqslant 0\} \text{ and } y(t) = (S(t),E(t),I(t),I_a(t),Q(t),I_h(t),I_c(t),R(t))^T.$$

Corollary 1. [24] *Suppose that $g(t) \in C[a,b]$ and ${}_a^{C}D_t^{\alpha}g(t) \in (a,b]$, where $\alpha \in (0,1]$. Then if*

$$(i). {}_a^{C}D_t^{\alpha}g(t) \geqslant 0, \forall\ y \in (a,b), \text{then } g(t) \text{ is non-decreasing.}$$

$$(ii). {}_a^{C}D_t^{\alpha}g(t) \leq 0, \forall\ y \in (a,b), \text{then } g(t) \text{ is non-increasing.}$$

3.5. Positivity and boundedness

.

Proposition 3.1. The solution of the system (6) is non-negative, bounded for all $(S(0),E(0),I(0),I_a(0),Q(0),I_h(0),I_c(0),R(0)) \in \mathbb{R}_+^8$, and also defined for all $t > 0$.

Proof. In order to explore the solution non-negativity, it is require to prove that on each hyperplane bounding the positive orthant, the vector

field point $\mathbb{R}^8_+$. Form the system (6) we obtained:

$$\begin{aligned}
{}^{C}D_t^{\alpha}S|_{S=0} &= \Lambda \geqslant 0, \quad {}^{C}D_t^{\alpha}E|_{E=0} = \lambda S \geqslant 0\\
{}^{C}D_t^{\alpha}I|_{I=0} &= \theta\omega E \geqslant 0, \quad {}^{C}D_t^{\alpha}I_a|_{I_a=0} = (1-\theta)\omega E \geqslant 0\\
{}^{C}D_t^{\alpha}Q|_{Q=0} &= \delta E \geqslant 0, \quad {}^{C}D_t^{\alpha}I_h|_{I_h=0} = \gamma I + \zeta Q \geqslant 0\\
{}^{C}D_t^{\alpha}I_c|_{I_c=0} &= \phi I_h \geqslant 0,\\
{}^{C}D_t^{\alpha}R|_{R=0} &= \vartheta_1 I + \vartheta_2 I_a + \phi_1 Q + \phi_2 I_h + \phi_3 I_c \geqslant 0.
\end{aligned}$$

Thus, by using the above corollary, the desire goal has been obtained i.e, the solution will stay in $\mathbb{R}^8_+$ and so, we can have the following region that biologically feasible:

$$\Xi = \left\{(S,E,I,I_a,Q,I_h,I_c,R) \in \mathbb{R}^8_+ : S,E,I,I_a,Q,I_h,I_c,R \geqslant 0.\right\}$$

Since all terms of the sum are positive, then the solution of system (6) is bounded.

Lemma 3.2. *The region Ξ is positively invariant for the model (6) with initial conditions in $\mathbb{R}^8_+$. Thus, it is enough to study the dynamics of the model in the region given in Ξ. This region can be assumed biologically and epidemiologically well-posed for our model considered.*

4. Analysis of the model

4.1. Disease-free equilibrium DFE

For the equilibrium points of the fractional model (6), we have

$${}^{C}D_t^{\alpha}S(t) = {}^{C}D_t^{\alpha}E(t) = {}^{C}D_t^{\alpha}I(t) = {}^{C}D_t^{\alpha}I_a(t) = {}^{C}D_t^{\alpha}Q(t) = {}^{C}D_t^{\alpha}I_h(t) = {}^{C}D_t^{\alpha}I_c(t) = {}^{C}D_t^{\alpha}R(t) = 0.$$

The DFE is denoted by $E_0^{**} = (S^0, E^0, I^0, I_a^0, Q^0, I_h^0, I_c^0, R^0)$ is as follow:

$$E_0^{**} = \left(\frac{\Lambda}{\mu}, 0, 0, 0, 0, 0, 0, 0\right). \tag{8}$$

4.2. The basic reproduction number

To derive the important threshold parameter also known is the basic reproduction number $\mathscr{R}_0$, by using the next-generation technique, for the dynamics of the disease, whether the infection in population is decaying or growing. Let $x = (E, I, I_a, Q, I_h, I_c)^T$, then we have

$$\frac{dx}{dt} = \mathscr{F} - \mathscr{V},$$

where

$$\mathscr{F} = \begin{pmatrix} \frac{\beta(I+\psi I_a+\tau I_c)S}{N} \\ 0 \\ 0 \\ 0 \\ 0 \\ 0 \end{pmatrix}, \quad \mathscr{V} = \begin{pmatrix} K_1 E \\ K_2 I - \theta\omega E \\ K_3 I_a - (1-\theta)\omega I_a \\ K_4 Q - \delta E \\ K_5 I_h - \gamma I - \zeta Q \\ K_6 I_c - \phi I_h \end{pmatrix}.$$

The Jacobian of above matrices for the linearized system at disease free-state is:

$$\mathbf{F} = \begin{pmatrix} 0 & \beta & \beta\psi & 0 & \beta\tau & 0 \\ 0 & 0 & 0 & 0 & 0 & 0 \\ 0 & 0 & 0 & 0 & 0 & 0 \\ 0 & 0 & 0 & 0 & 0 & 0 \\ 0 & 0 & 0 & 0 & 0 & 0 \\ 0 & 0 & 0 & 0 & 0 & 0 \end{pmatrix}, \quad \mathbf{V} = \begin{pmatrix} K_1 & 0 & 0 & 0 & 0 & 0 \\ -\theta\omega & K_2 & 0 & 0 & 0 & 0 \\ -(1-\theta)\omega & 0 & K_3 & 0 & 0 & 0 \\ -\delta & 0 & 0 & K_4 & 0 & 0 \\ 0 & -\gamma & 0 & -\zeta & K_5 & 0 \\ 0 & 0 & 0 & 0 & -\phi & K_6 \end{pmatrix}.$$

Hence the next-generation matrix is obtained as

$$\mathbf{FV}^{-1} = \begin{pmatrix} \frac{\beta\theta\omega}{K_1K_2} + \frac{\beta\tau(K_2\delta\zeta + K_4\gamma\theta\omega)}{K_1K_2K_4K_5} + \frac{\beta\psi\omega(1-\theta)}{K_1K_3} & \frac{\beta}{K_2} + \frac{\beta\tau\gamma}{K_2K_5} & \frac{\beta\psi}{K_3} & \frac{\beta\tau\zeta}{K_4K_5} & \frac{\beta\tau}{K_5} & 0 \\ 0 & 0 & 0 & 0 & 0 & 0 \\ 0 & 0 & 0 & 0 & 0 & 0 \\ 0 & 0 & 0 & 0 & 0 & 0 \\ 0 & 0 & 0 & 0 & 0 & 0 \\ 0 & 0 & 0 & 0 & 0 & 0 \end{pmatrix}.$$

The basic reproduction number $\mathscr{R}_0$ at DFE is obtained by taking the spectral radius of the Next-generation matrix $\rho(\mathbf{FV}^{-1})$ for fractional model as follow:

$$\mathscr{R}_0 = \frac{\beta[K_2K_3\delta\zeta\tau + K_4\omega(K_3\theta(K_5+\tau\gamma) + K_2K_5\psi(1-\theta))]}{K_1K_2K_3K_4K_5}. \tag{9}$$

4.3. Local stability of DFE

.

Theorem 4.1. *Let $m > 0$ and $n > 0$ are the integers such that $gcd(m,n) = 1$ for $\alpha = \frac{m}{n}$ and $M = n$, then the DFE of the model in fractional derivative is locally asymptotically stable if $|arg(\lambda)| > \frac{\pi}{2M}$ for all roots λ of the associated characteristic equation,*

$$det(diag[\lambda^{M\alpha}\lambda^{M\alpha}\lambda^{M\alpha}\lambda^{M\alpha}\lambda^{M\alpha}\lambda^{M\alpha}] - J(E_0^{**})) = 0. \tag{10}$$

Proof. For local stability, the linearized system is the jacobian of system (6) at E_0^{**} implies that:

$$J(E_0^{**}) = \begin{pmatrix} -\mu & 0 & -\beta & -\beta\psi & 0 & -\beta\tau & 0 & 0 \\ 0 & -K_1 & \beta & \beta\psi & 0 & \beta\tau & 0 & 0 \\ 0 & \theta\omega & -K_2 & 0 & 0 & 0 & 0 & 0 \\ 0 & (1-\theta)\omega & 0 & -K_3 & 0 & 0 & 0 & 0 \\ 0 & \delta & 0 & 0 & -K_4 & 0 & 0 & 0 \\ 0 & 0 & \gamma & 0 & \zeta & -K_5 & 0 & 0 \\ 0 & 0 & 0 & 0 & 0 & \phi & -K_6 & 0 \\ 0 & 0 & \vartheta_1 & \vartheta_2 & \phi_1 & \phi_2 & \phi_3 & -\mu \end{pmatrix}.$$

After the evaluation of determinant Eq. (10) implies,

$$(\lambda^m + \mu_0)^2(\lambda^m + K_6)(\lambda^{5m} + a_1\lambda^{4m} + a_2\lambda^{3m} + a_3\lambda^{2m} + a_4\lambda^m + a_5) = 0, \tag{11}$$

here we can say that the three eigen values are $-\mu, -\mu, -K_6$ have negative or negative real part and the co-efficient mentioned above is of the form

$$
\begin{aligned}
a_1 &= K_1+K_2+K_3+K_4+K_5,\\
a_2 &= K_1K_2+K_1K_3+K_2K_3+K_1K_4+K_2K_4+K_3K_4+K_1K_5+K_2K_5+K_3K_5\\
&\quad +K_4K_5-\beta\omega(\theta+\psi(1-\theta)),\\
a_3 &= K_1K_2K_3+K_1K_2K_4+K_1K_3K_4+K_2K_3K_4+K_1K_2K_5+K_1K_3K_5+K_2K_3K_5\\
&\quad +K_1K_4K_5+K_2K_4K_5+K_3K_4K_5-\beta\theta\omega(\gamma\vartheta+K_3+K_4+K_5)-\beta\tau\delta\zeta\\
&\quad -\beta\psi\omega(1-\theta)(K_2+K_4+K_5),\\
a_4 &= K_1K_2K_3K_4+K_1K_2K_3K_5+K_1K_2K_4K_5+K_1K_3K_4K_5+K_2K_3K_4K_5\\
&\quad -\beta\theta\omega\gamma\tau(K_3+K_4)-\beta\tau\delta\zeta(K_2+K_3)-\beta\psi\omega(1-\theta)(K_2K_4+K_2K_5+K_4K_5),\\
a_5 &= K_1K_2K_3K_4K_5-\beta[\delta\zeta K_2K_3\tau+K_4\omega(K_3\theta(K_5+\gamma\tau)+K_2K_5\psi(1-\theta))],\\
&= K_1K_2K_3K_4K_5(1-\mathscr{R}_0).
\end{aligned}
$$

Clearly, a_i are all positive if $\mathscr{R}_0<1$. The argument of the root of equation $(\lambda^m+\mu)^2=0$ and $(\lambda^m+K_6)=0$ are similar, that is:

$$arg(\lambda_k)=\frac{\pi}{m}+k\frac{2\pi}{m}>\frac{\pi}{M}>\frac{\pi}{2M},\quad where\ \ k=0,1,2,\ldots,(m-1).$$

In similar fashion, we find out the arguments of the roots of equation $(\lambda^{5m}+a_1\lambda^{4m}+a_2\lambda^{3m}+a_3\lambda^{2m}+a_4\lambda^m+a_5)=0$ are all greater than $\frac{\pi}{2M}$ if $\mathscr{R}_0<1$, having an argument less than $\frac{\pi}{2M}$ for $\mathscr{R}_0>1$. Thus the DFE is locally asymptotically stable for $\mathscr{R}_0<1$.

Lemma 4.1. *The disease-free equilibrium of the system (6) is unstable if* $\mathscr{R}_0>1$.

4.4. Global stability of DFE

To show global asymptotic stability (GAS) of DFE E_0^{**} of the model (6) by Layapunov function approach, we proceed as in the following result.

Theorem 4.2. *If* $\mathscr{R}_0\leqslant 1$ *then* DFE *of the Caputo COVID-19 model given by (8) is* GAS.

Proof. Let the Lyapunov function be in the form below:

$$\Im(E,I,I_a,Q,I_h)=\left(\frac{\mathscr{R}_0K_5}{\beta\tau}\right)E+\left(\frac{K_5+\tau\gamma}{K_2\tau}\right)I+\left(\frac{K_5\psi}{K_3\tau}\right)I_a+\left(\frac{\zeta}{K_4}\right)Q+I_h.$$

The Caputo fractional derivative of $\Im(E,I,I_a,Q,I_h)$, along model (6) satisfies:

$$
\begin{aligned}
{}^{C}D_t^{\alpha}\Im(E,I,I_a,Q,I_h) &= \left(\frac{\mathscr{R}_0K_5}{\beta\tau}\right){}^{C}D_t^{\alpha}E+\left(\frac{K_5+\tau\gamma}{K_2\tau}\right){}^{C}D_t^{\alpha}I+\left(\frac{K_5\psi}{K_3\tau}\right){}^{C}D_t^{\alpha}I_a\\
&\quad +\left(\frac{\zeta}{K_4}\right){}^{C}D_t^{\alpha}Q+{}^{C}D_t^{\alpha}I_h,\\
&= \frac{\mathscr{R}_0K_5}{\beta\tau}\left[\frac{\beta S(I+\psi I_a+\tau I_h)}{N}-K_1E\right]+\left(\frac{K_5+\tau\gamma}{K_2\tau}\right)\left(\theta\omega E-K_2I\right)\\
&\quad +\left(\frac{K_5\psi}{K_3\tau}\right)((1-\theta)\omega E-K_3I_a)+\left(\frac{\zeta}{K_4}\right)\left(\delta E-K_4Q\right)+\gamma I\\
&\quad +\zeta Q-K_5I_h,\\
&\leqslant \frac{\mathscr{R}_0K_5}{\beta\tau}[\beta(I+\psi I_a+\tau I_h)-K_1E]+\left(\frac{K_5+\tau\gamma}{K_2\tau}\right)\left(\theta\omega E-K_2I\right)\\
&\quad +\left(\frac{K_5\psi}{K_3\tau}\right)\left((1-\theta)\omega E-K_3I_a\right)+\left(\frac{\zeta}{K_4}\right)\left(\delta E-K_4Q\right)+\gamma I\\
&\quad +\zeta Q-K_5I_h,\ S\leqslant N.\\
&= \left(\frac{\mathscr{R}_0K_5}{\tau}I-\frac{K_5}{\tau}I\right)+\left(\frac{\mathscr{R}_0K_5}{\tau}\psi I_a-\frac{K_5}{\tau}\psi I_a\right)+(\mathscr{R}_0K_5I_h-K_5I_h)\\
&\quad +\left(\frac{\delta\zeta}{K_4}-\frac{\mathscr{R}_0K_5K_1}{\beta\tau}E+(\frac{K_5+\tau\gamma}{K_2\tau})\theta\omega E+\frac{\psi K_5}{K_3\tau}(1-\theta)\omega E\right),\\
&= \frac{K_5}{\tau}(\mathscr{R}_0-1)I+\frac{K_5}{\tau}(\mathscr{R}_0-1)\psi I_a+K_5(\mathscr{R}_0-1)I_h,\\
&\leqslant \frac{K_5}{\tau}(\mathscr{R}_0-1)(I+\psi I_a+\tau I_h),\\
&\leqslant 0.
\end{aligned}
$$

Hence, it follows that ${}^{C}D_t^{\alpha}\Im\leq 0$, for $\mathscr{R}_0<1$ all the parameters and variables are non-negative with ${}^{C}D_t^{\alpha}\Im=0$ iff $E=I=I_a=Q=I_h=0$. So the infected compartments (E,I,I_a,Q,I_h) approached zero whenever $t\to\infty$. Using $E=I=I_a=Q=I_h=0$ in equations of system (6), we have $S\to\frac{\Lambda}{\mu},I_c\to 0$ and $R\to 0$ as $t\to\infty$. Thus using lypaunov stability theorems for fractional case developed in [37], every solution of the Caputo model (6) with non-negative initial conditions, approaches to E_0^{**} as $t\to\infty$ in Ξ. Thus, it follows that the DFE of the model (6) is GAS. In the next subsections, we have to explore the positive equilibria of the model where at least one of the infected component is non-zero.

4.5. Existence of endemic equilibrium point

The arbitrary endemic equilibrium point (EEP) for the Caputo model (6), represented by

$$E_1^{**}=(S^{**},E^{**},I^{**},I_a^{**},Q^{**},I_h^{**},I_c^{**},R^{**})$$

with $N^{**}=(S^{**}+E^{**}+I^{**}+I_a^{**}+Q^{**}+I_h^{**}+I_c^{**}+R^{**})$. Now at steady state, after solving the equations of Caputo model gives

$$
\begin{aligned}
S^{**} &= \frac{\Lambda}{\lambda^{*}+\mu},\\
E^{**} &= \frac{\lambda^{*}\Lambda}{K_1(\lambda^{*}+\mu)} = \frac{\lambda^{*}S^{**}}{K_1},\\
I^{**} &= \frac{\theta\omega\lambda^{*}\Lambda}{K_1K_2(\lambda^{*}+\mu)} = \frac{\theta\omega E^{**}}{K_2} = \frac{\theta\omega\lambda^{*}S^{**}}{K_1K_2} = d_1\lambda^{*}S^{**},\\
I_a^{**} &= \frac{(1-\theta)\omega\lambda^{*}\Lambda}{K_1K_3(\lambda^{*}+\mu)} = \frac{(1-\theta)\omega E^{**}}{K_3} = \frac{(1-\theta)\omega\lambda^{*}S^{**}}{K_1K_3} = d_2\lambda^{*}S^{**},\\
Q^{**} &= \frac{\delta\lambda^{*}\Lambda}{K_1K_4(\lambda^{*}+\mu)} = \frac{\delta E^{**}}{K_4} = \frac{\delta\lambda^{*}S^{**}}{K_1K_4} = d_3\lambda^{*}S^{**},\\
I_h^{**} &= \frac{\gamma I^{**}+\zeta Q^{**}}{K_5} = (K_4\gamma\theta\omega+K_2\delta\zeta)\frac{E^{**}}{K_2K_4K_5} = (K_4\gamma\theta\omega+K_2\delta\zeta)\frac{\lambda^{*}S^{**}}{K_1K_2K_4K_5},\\
I_c^{**} &= \frac{\phi I_h^{**}}{K_6} = \phi\frac{\gamma I^{**}+\zeta Q^{**}}{K_5K_6} = \phi(K_4\gamma\theta\omega+K_2\delta\zeta)\frac{\lambda^{*}S^{**}}{K_1K_2K_4K_5K_6} = \frac{\phi d_4\lambda^{*}S^{**}}{K_6},\\
R^{**} &= \frac{1}{\mu}\left(\vartheta_1 I^{**}+\vartheta_2 I_a^{**}+\phi_1 Q^{**}+\phi_2 I_h^{**}+\phi_3 I_c^{**}\right) = \frac{d_5\lambda^{*}S^{**}}{\mu}.
\end{aligned}
\tag{12}
$$

Further, we define the force of infection at endemic state as below:

$$
\lambda^{*} = \frac{\beta(I^{**}+\psi I_a^{**}+\tau I_h^{**})}{N^{**}}. \tag{13}
$$

substituting (12) in (13), we have

$$
\lambda^{*} = \frac{\beta\left(\frac{\theta\omega\lambda^{*}S^{**}}{K_1K_2}+\psi\frac{(1-\theta)\omega\lambda^{*}S^{**}}{K_1K_3}+\tau(K_4\gamma\theta\omega+K_2\delta\zeta)\frac{\lambda^{*}S^{**}}{K_1K_2K_4K_5}\right)}{N^{**}},
$$

after simplification, we get

$$
(\lambda^{*}+\mu)N^{**} = \Lambda\mathscr{R}_0,
$$

Hence,

$$
\lambda^{*} = \frac{\mathscr{R}_0-1}{d_6} > 0, \quad \mathscr{R}_0 > 1,
$$

where,

$$
d_6 = \frac{1}{K_1}+d_1+d_2+d_3+d_4+\frac{\phi d_4}{K_6}+\frac{d_5}{\mu}.
$$

Lemma 4.2. *There exists a unique endemic state for the model (6), whenever $\mathscr{R}_0 > 1$.*

4.6. Local stability of (EEP)

To formulate the Jacobian of system (6) at endemic state. The following result is obtained as:

Theorem 4.3. *The endemic equilibrium E_1^{**} of Caputo-fractional model (6) along with $N = N^{**}$ is (LAS), if $\mathscr{R}_0 > 1$.*

Proof. The Jacobian of system (6) at associated endemic equilibrium (EE) follows that;

$$
J(E_1^{**}) = [U_{4\times8}V_{4\times8}],
$$

where,

$$
U = \begin{pmatrix}
-\mu+\frac{S^{**}\lambda^{*}}{(N^{**})^2}-\frac{\lambda^{*}}{N^{**}} & \frac{S^{**}\lambda^{*}}{(N^{**})^2} & -\frac{\beta S^{**}}{N^{**}}+\frac{S^{**}\lambda^{*}}{(N^{**})^2}-\frac{\beta\psi S^{**}}{N^{**}}+\frac{S^{**}\lambda^{*}}{(N^{**})^2}\\
-\frac{S^{**}\lambda^{*}}{(N^{**})^2}+\frac{\lambda^{*}}{N^{**}} & -K_1-\frac{S^{**}\lambda^{*}}{(N^{**})^2} & \frac{\beta S^{**}}{N^{**}}-\frac{S^{**}\lambda^{*}}{(N^{**})^2} & \frac{\beta\psi S^{**}}{N^{**}}-\frac{S^{**}\lambda^{*}}{(N^{**})^2}\\
0 & \theta\omega & -K_2 & 0\\
0 & (1-\theta)\omega & 0 & -K_3\\
0 & \delta & 0 & 0\\
0 & 0 & \gamma & 0\\
0 & 0 & 0 & 0\\
0 & 0 & \vartheta_1 & \vartheta_2
\end{pmatrix},
$$

and

$$
V = \begin{pmatrix}
\frac{S^{**}\lambda^{*}}{(N^{**})^2} & -\frac{\beta\tau S^{**}}{N^{**}}+\frac{S^{**}\lambda^{*}}{(N^{**})^2} & \frac{S^{**}\lambda^{*}}{(N^{**})^2} & \frac{S^{**}\lambda^{*}}{(N^{**})^2}\\
-\frac{S^{**}\lambda^{*}}{(N^{**})^2} & \frac{\beta\tau S^{**}}{N^{**}}-\frac{S^{**}\lambda^{*}}{(N^{**})^2} & -\frac{S^{**}\lambda^{*}}{(N^{**})^2} & -\frac{S^{**}\lambda^{*}}{(N^{**})^2}\\
0 & 0 & -0 & 0\\
0 & 0 & 0 & 0\\
-K_4 & 0 & 0 & 0\\
\zeta & -K_5 & 0 & 0\\
0 & \phi & -K_6 & 0\\
\phi_1 & \phi_2 & \phi_3 & -\mu
\end{pmatrix},
$$

One of the eigenvalue is $-\mu$, that is negative and others can be obtained from the equation:

$$
\lambda^7+b_1\lambda^6+b_2\lambda^5+b_3\lambda^4+b_4\lambda^3+b_5\lambda^2+b_6\lambda+b_7 = 0. \tag{14}
$$

Now the Hurwitz matrices are:

$$
H_1 = b_1, \quad H_2 = \begin{pmatrix} b_1 & 1\\ b_3 & b_2 \end{pmatrix},
$$

$$
H_3 = \begin{pmatrix} b_1 & 1 & 0\\ b_3 & b_2 & b_1\\ b_5 & b_4 & b_3 \end{pmatrix}, \quad H_4 = \begin{pmatrix} b_1 & 1 & 0 & 0\\ b_3 & b_2 & 1 & 0\\ b_5 & b_4 & b_3 & b_2\\ 0 & 0 & b_5 & b_4 \end{pmatrix}, \quad H_5 = \begin{pmatrix} b_1 & 1 & 0 & 0 & 0\\ b_3 & b_2 & b_1 & 1 & 0\\ b_5 & b_4 & b_3 & b_2 & b_1\\ 0 & 0 & b_5 & b_4 & b_3\\ 0 & 0 & 0 & 0 & b_5 \end{pmatrix},
$$

$$
H_6 = \begin{pmatrix} b_1 & 1 & 0 & 0 & 0 & 0\\ b_3 & b_2 & b_1 & 1 & 0 & 0\\ b_5 & b_4 & b_3 & b_2 & b_1 & 1\\ 0 & 0 & b_5 & b_4 & b_3 & b_2\\ 0 & 0 & 0 & 0 & b_5 & b_4\\ 0 & 0 & 0 & 0 & 0 & b_6 \end{pmatrix}, \quad H_7 = \begin{pmatrix} b_1 & 1 & 0 & 0 & 0 & 0 & 0\\ b_3 & b_2 & b_1 & 1 & 0 & 0 & 0\\ b_5 & b_4 & b_3 & b_2 & b_1 & 1 & 0\\ 0 & 0 & b_5 & b_4 & b_3 & b_2 & b_1\\ 0 & 0 & 0 & 0 & b_5 & b_4 & b_3\\ 0 & 0 & 0 & 0 & 0 & b_6 & b_5\\ 0 & 0 & 0 & 0 & 0 & 0 & b_7 \end{pmatrix},
$$

Here we can say that the coefficient signs b_j are strictly positive for the roots of the polynomial to be negative. All roots of polynomial have negative real part iff, Det$H_j > 0$, $j = 1, 2, \ldots, 7$. Thus, the conditions ensures the endemic stability.

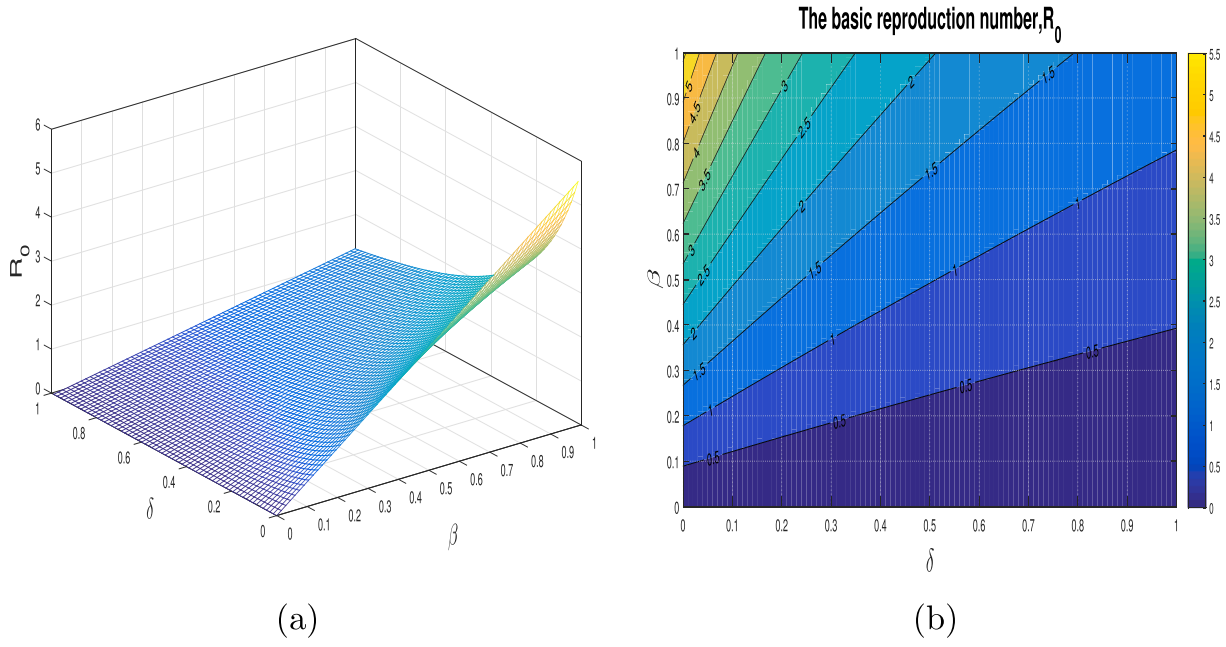

Fig. 3. Impact of effective contact rate β and quarantine rate δ on $\mathscr{R}_0$ with contour plot.

4.7. Global stability of EEP

For global stability at endemic state of the Caputo COVID-19 model (6) is given for the special case when infected hospitalized do not transmit infection ($\tau = 0$), and disease-induced mortality is negligible ($\xi_1 = \xi_2 = 0$), then the reduced model is obtained as:

$$\begin{cases} {}^{C}D_t^{\alpha}S(t) = \Lambda - \dfrac{\beta(I+\psi I_a+\tau I_h)}{N}S - \mu S, \\ {}^{C}D_t^{\alpha}E(t) = \dfrac{\beta(I+\psi I_a+\tau I_h)}{N}S - (\omega+\delta+\mu)E, \\ {}^{C}D_t^{\alpha}I(t) = \theta\omega E - (\vartheta_1+\mu+\gamma)I, \\ {}^{C}D_t^{\alpha}I_a(t) = (1-\theta)\omega E - (\vartheta_2+\mu)I_a, \\ {}^{C}D_t^{\alpha}Q(t) = \delta E - (\mu+\phi_1+\zeta)Q, \\ {}^{C}D_t^{\alpha}I_h(t) = \gamma I + \zeta Q - (\mu+\phi_2+\phi)I_h, \\ {}^{C}D_t^{\alpha}I_c(t) = \phi I_h - (\mu+\phi_3+\xi_3)I_c, \\ {}^{C}D_t^{\alpha}R(t) = \vartheta_1 I + \vartheta_2 I_a + \phi_1 Q + \phi_2 I_h + \phi_3 I_c - \mu R, \end{cases} \tag{15}$$

where, now

$$\lambda(t) = \frac{\beta(I+\psi I_a)}{N}$$

The reduced model shows that $N(t)\to\frac{\Lambda}{\mu}$as $t\to\infty$. Finally we have

$$\lambda_1(t) = \beta_1(I+\psi I_a), \quad \beta_1 = \frac{\beta\mu}{\Lambda}. \tag{16}$$

The relative expression for the reproduction number $\mathscr{R}_{01}$ of the reduced model with (16) is

$$\mathscr{R}_{01} = \frac{\beta_1\omega[K_3\theta + k_2\psi(1-\theta)]}{K_1k_2K_3}. \tag{17}$$

The following results for model (15) at steady state obtained as:

$$\begin{cases} \Lambda &= (\lambda_1^* + \mu)S^{***}, \\ K_1E^{***} &= \lambda_1^*S^{***}, \\ k_2I^{***} &= \theta\omega E^{***}, \\ K_3I_a^{***} &= (1-\theta)\omega E^{***}. \end{cases} \tag{18}$$

$$\lambda_1^* = \beta_1(I^{***} + \psi I_a^{***}), \quad k_2 = \vartheta_1 + \mu + \gamma.$$

Theorem 4.4. *The fractional model (15) at unique* EEP *i.e.,* E_1^{***} *is* GAS *in* Ξ*, if* $\mathscr{R}_{01} > 1$ *and the condition (25) holds.*

Proof. Consider the following non-linear Lyapunov function for the model (15), so that the corresponding unique EEP E_1^{***} exist by letting $\mathscr{R}_{01} > 1$.

$$\begin{aligned} \Re(t) = &\left(S(t) - S^{***} - S^{***}\ln\frac{S(t)}{S^{***}}\right) + \left(E(t) - E^{***} - E^{***}\ln\frac{E(t)}{E^{***}}\right) \\ &+ \frac{K_1}{\theta\omega}\left(I(t) - I^{***} - I^{***}\ln\frac{I(t)}{I^{***}}\right) + \frac{K_1}{(1-\theta)\omega}\left(I_a(t) - I_a^{***} - I_a^{***}\ln\frac{I_a(t)}{I_a^{***}}\right) \end{aligned} \tag{19}$$

The time fractional derivative of (19) is:

$$\begin{aligned} {}^{C}D_t^{\alpha}\Re(t) = &\left(1-\frac{S^{***}}{S}\right){}^{C}D_t^{\alpha}S(t) + \left(1-\frac{E^{***}}{E}\right){}^{C}D_t^{\alpha}E(t) + \frac{K_1}{\theta\omega}\left(1-\frac{I^{***}}{I}\right){}^{C}D_t^{\alpha}I(t) \\ &+ \frac{K_1}{(1-\theta)\omega}\left(1-\frac{I_a^{***}}{I_a}\right){}^{C}D_t^{\alpha}I_a(t), \\ = &\left(1-\frac{S^{***}}{S}\right)(\Lambda - \lambda_1 S - \mu S) + \left(1-\frac{E^{***}}{E}\right)(\lambda_1 S - K_1 E) \\ &+ \frac{K_1}{\theta\omega}\left(1-\frac{I^{***}}{I}\right)(\theta\omega E - k_2 I) + \frac{K_1}{(1-\theta)\omega}\left(1-\frac{I_a^{***}}{I_a}\right)((1-\theta)\omega E - K_3 I_a). \end{aligned}$$

Using the solution from (18) gives

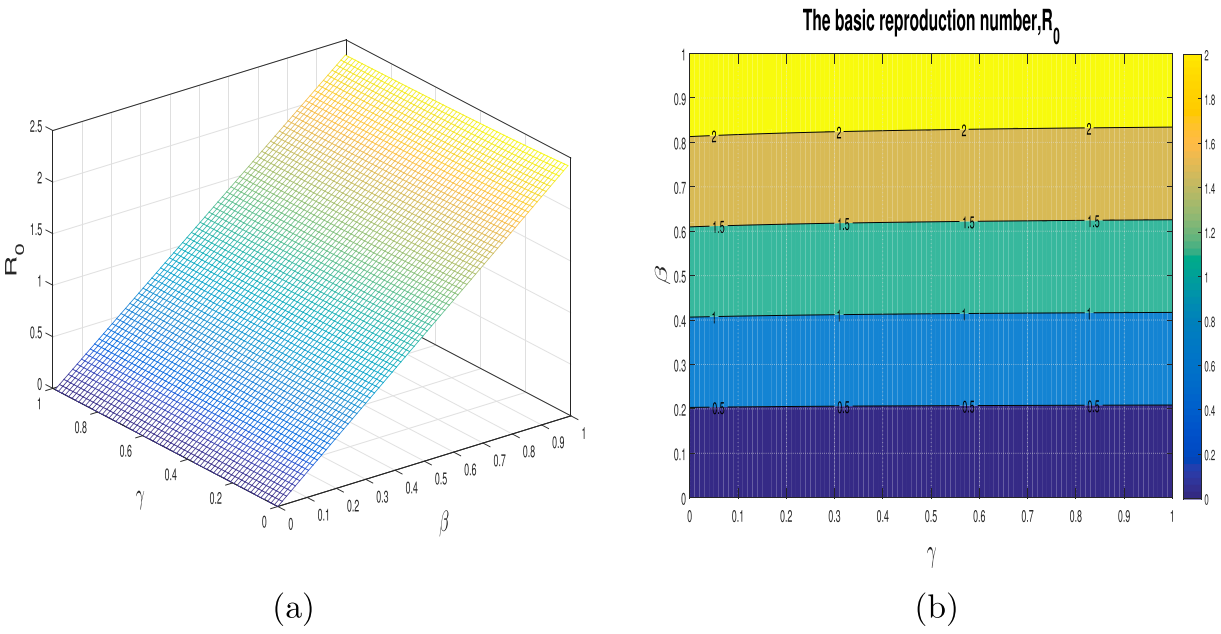

Fig. 4. Impact of effective contact rate β and hospitalization/self-isolation rate γ on $\mathscr{R}_0$ with contour plot.

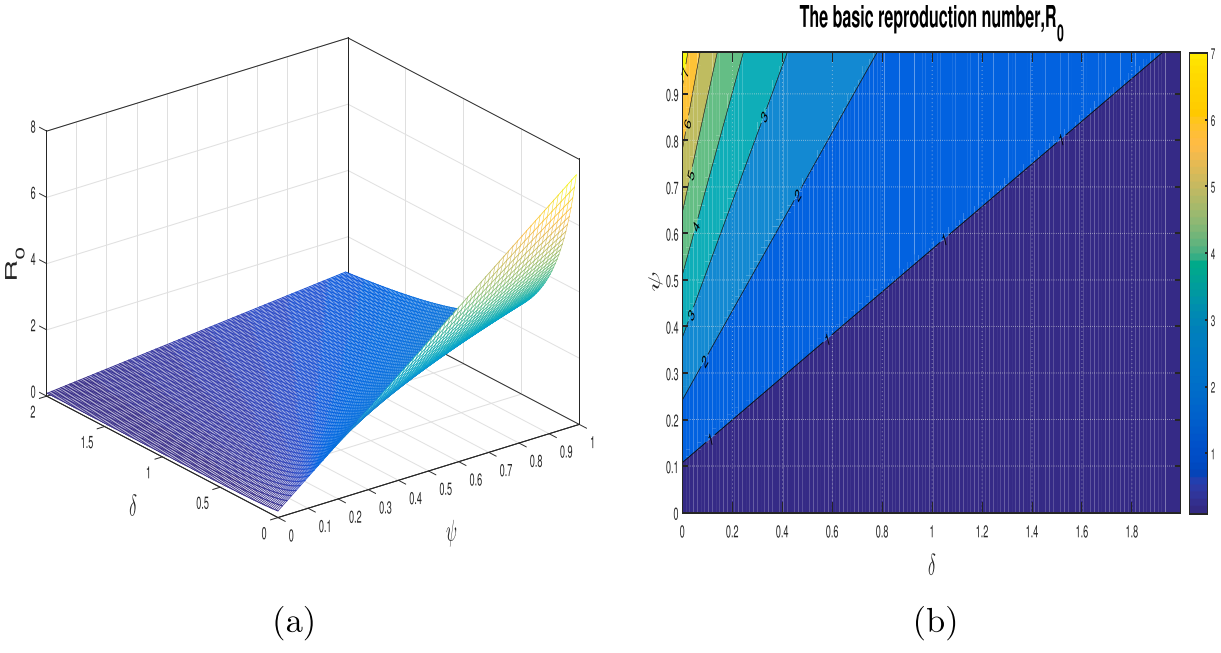

Fig. 5. Impact of transmission coefficient ψ and quarantined rate δ on the basic reproduction number $\mathscr{R}_0$ with contour plot.

$$\left(1-\frac{S^{***}}{S}\right){}^{C}D_t^{\alpha}S(t)=\left(1-\frac{S^{***}}{S}\right)\left((\beta_1(I^{***}+\psi I_a^{***})+\mu)S^{***}-\beta_1(I+\psi I_a)S-\mu S\right),$$
$$=\beta_1 S^{***}I^{***}\left(1-\frac{S^{***}}{S}-\frac{IS}{I^{***}S^{***}}+\frac{I}{I^{***}}\right)$$
$$+\beta_1\psi S^{***}I_a^{***}\left(1-\frac{S^{***}}{S}-\frac{I_aS}{I_a^{***}S^{***}}+\frac{I_a}{I_a^{***}}\right)$$
$$+\mu S^{***}\left(2-\frac{S^{***}}{S}-\frac{S}{S^{***}}\right).$$
(20)

$$\left(1-\frac{E^{***}}{E}\right){}^{C}D_t^{\alpha}E(t)=\left(1-\frac{E^{***}}{E}\right)\left(\beta_1(I+\psi I_a)S-\beta_1(I^{***}S^{***}+\psi I_a^{***}S^{***})\frac{E}{E^{***}}\right)$$
$$=\beta_1 S^{***}I^{***}\left(1-\frac{E}{E^{***}}-\frac{E^{***}IS}{EI^{***}S^{***}}+\frac{IS}{I^{***}S^{***}}\right)$$
$$+\beta_1\psi S^{***}I_a^{***}\left(1-\frac{E}{E^{***}}-\frac{E^{***}I_aS}{EI_a^{***}S^{***}}+\frac{I_aS}{I_a^{***}S^{***}}\right).$$
(21)

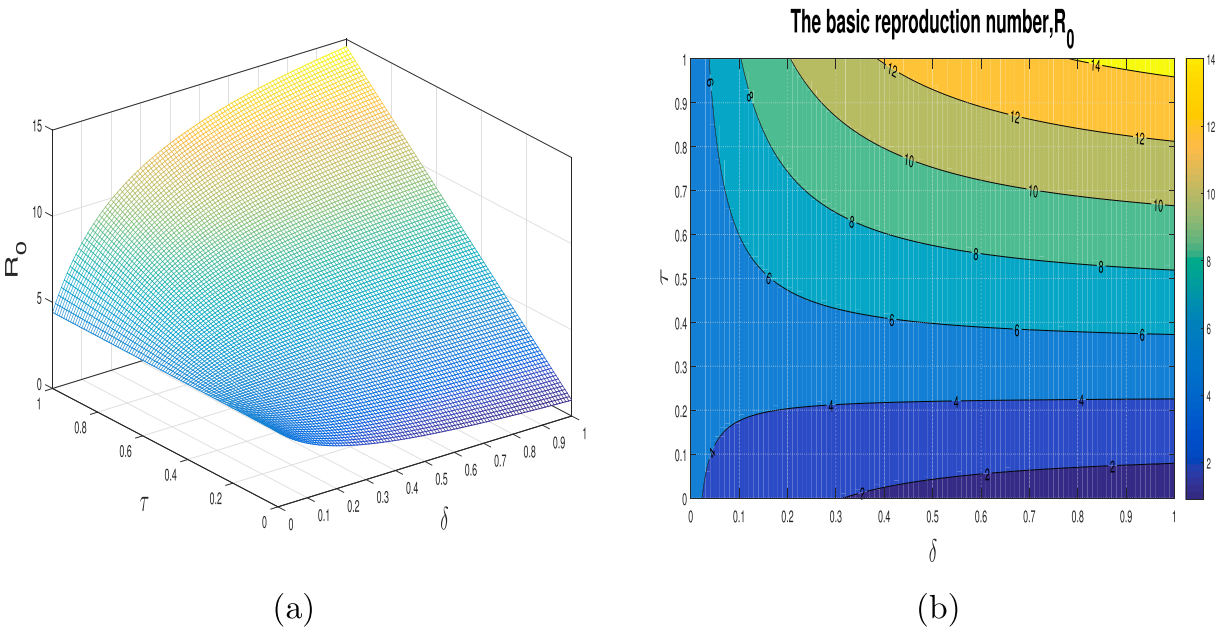

Fig. 6. Effect of transmission coefficient τ and quarantined rate δ on the basic reproduction number $\mathscr{R}_0$ with corresponding contour plot.

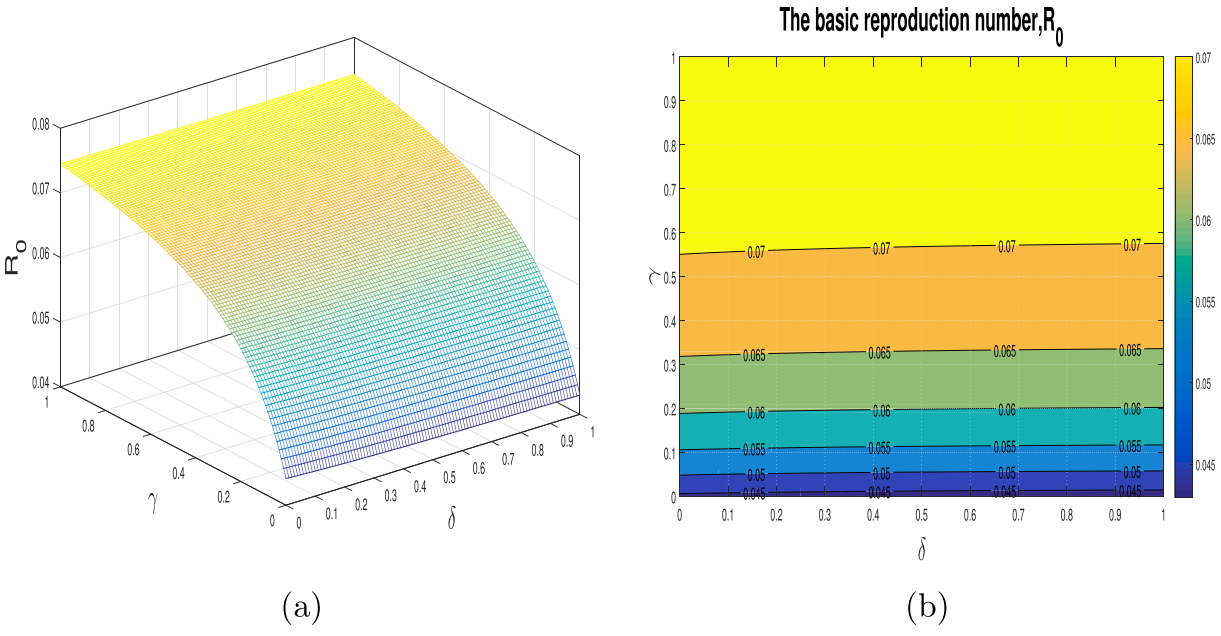

Fig. 7. Effect of hospitalization/self-isolation γ and quarantined rate δ on the basic reproduction number $\mathscr{R}_0$ with corresponding contour plot.

$$\begin{aligned}\left(\frac{K_1}{\theta\omega}\right)\left(1-\frac{I^{***}}{I}\right){}^{C}D_t^{\alpha}I(t) &= \left(\frac{K_1}{\theta\omega}\right)\left(1-\frac{E^{***}}{E}\right)\left(\theta\omega E-\theta\omega E^{***}\frac{I}{I^{***}}\right),\\ &= K_1E^{***}\left(1-\frac{I}{I^{***}}-\frac{I^{***}E}{IE^{***}}+\frac{E}{E^{***}}\right),\\ &= \beta_1S^{***}I^{***}\left(1-\frac{I}{I^{***}}-\frac{I^{***}E}{IE^{***}}+\frac{E}{E^{***}}\right)\\ &\quad+\beta_1\psi S^{***}I_a^{***}\left(1-\frac{I}{I^{***}}-\frac{I^{***}E}{IE^{***}}+\frac{E}{E^{***}}\right).\end{aligned} \tag{22}$$

$$\begin{aligned}\left(\frac{K_1}{\omega(1-\theta)}\right)\left(1-\frac{I_a^{***}}{I_a}\right){}^{C}D_t^{\alpha}I_a(t) &= \left(\frac{K_1}{\omega(1-\theta)}\right)\left(\omega(1-\theta)E-\omega(1-\theta)E^{***}\frac{I_a}{I_a^{***}}\right),\\ &= \lambda_1^{*}S^{***}\left(1-\frac{I_a}{I_a^{***}}-\frac{I_a^{***}E}{I_aE^{***}}+\frac{E}{E^{***}}\right),\\ &= \beta_1S^{***}I_a^{***}\left(1-\frac{I_a}{I_a^{***}}-\frac{I_a^{***}E}{I_aE^{***}}+\frac{E}{E^{***}}\right)\\ &\quad+\beta_1\psi S^{***}I_a^{***}\left(1-\frac{I_a}{I_a^{***}}-\frac{I_a^{***}E}{I_aE^{***}}+\frac{E}{E^{***}}\right).\end{aligned} \tag{23}$$

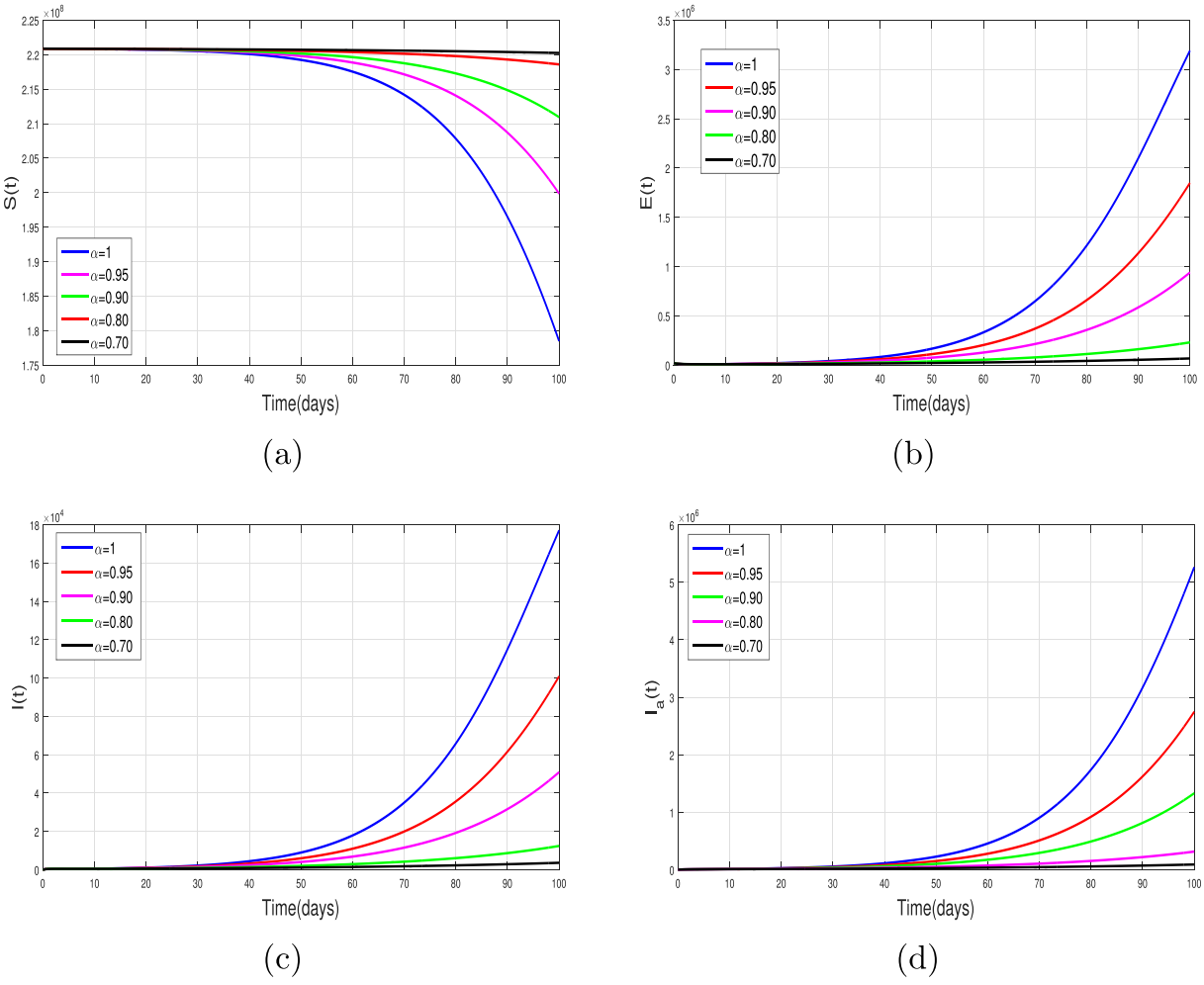

Fig. 8. Dynamics of fractional COVID-19 model for different values of α.

Substitute (20) to (23) in (20), after simplification gives

$$
\begin{aligned}
{}^{C}D_t^{\alpha}\Re(t) = {} & \beta_1 S^{***} I_a^{***}\left(4-\frac{S^{***}}{S}-\frac{I_a}{I_a^{***}}-\frac{E^{***}IS}{EI^{***}S^{***}}-\frac{I^{***}E}{IE^{***}}-\frac{I_a^{***}E}{I_aE^{***}}+\frac{E}{E^{***}}\right)\\
& +\beta_1\psi S^{***} I_a^{***}\left(4-\frac{S^{***}}{S}-\frac{I}{I^{***}}-\frac{E^{***}I_aS}{EI_a^{***}S^{***}}-\frac{I^{***}E}{IE^{***}}-\frac{I_a^{***}E}{I_aE^{***}}+\frac{E}{E^{***}}\right)\\
& +\mu S^{***}\left(2-\frac{S^{***}}{S}-\frac{S}{S^{***}}\right).
\end{aligned}
\tag{24}
$$

Since the arithmetic mean exceeds the geometric mean, we have the following interpretation form (24):

$$
\left(2-\frac{S^{***}}{S}-\frac{S}{S^{***}}\right) = -\frac{(S-S^{***})^2}{SS^{***}} \le 0.
$$

Further, if the following inequalities holds

$$
\begin{cases}
\left(4-\dfrac{S^{***}}{S}-\dfrac{I_a}{I_a^{***}}-\dfrac{E^{***}IS}{EI^{***}S^{***}}-\dfrac{I^{***}E}{IE^{***}}-\dfrac{I_a^{***}E}{I_aE^{***}}+\dfrac{E}{E^{***}}\right)\le 0,\\
\left(4-\dfrac{S^{***}}{S}-\dfrac{I}{I^{***}}-\dfrac{E^{***}I_aS}{EI_a^{***}S^{***}}-\dfrac{I^{***}E}{IE^{***}}-\dfrac{I_a^{***}E}{I_aE^{***}}+\dfrac{E}{E^{***}}\right)\le 0,
\end{cases}
\tag{25}
$$

then ${}^{C}D_t^{\alpha}\Re(t) \le 0$ for $\mathscr{R}_{01}$. Thus, $\Re(t)$ is a Lyaponov function in Ξ. Therefore, by Lasalle invariance principle, that

$$
\begin{aligned}
\lim_{t\to\infty} S(t) = S^{***}, \ \lim_{t\to\infty} E(t) = E^{***}, \ \lim_{t\to\infty} I(t) = I^{***}, \ \lim_{t\to\infty} I_a(t)\\
= I_a^{***}, \lim_{t\to\infty} Q(t) = Q^{***}, \ \lim_{t\to\infty} I_h(t) = I_h^{***}, \ \lim_{t\to\infty} I_c(t)\\
= I_c^{***}, \ \lim_{t\to\infty} R(t) = R^{***}.
\end{aligned}
$$

Thus every solution of the reduced model, tends to its unique endemic equilibrium for associated reproduction number as $t\to\infty$. For the GAS of EEP (E_1^{**}) whenever $\mathscr{R}_0 > 1$, through the conjecture.

Remark 1. The unique EEP of system (6) is GAS in Ξ, if $\mathscr{R}_0 > 1$, in Ξ.

5. $\mathscr{R}_0$ versus model parameters

Figs. 3–7 depict the impact of model various important parameters on the value of $\mathscr{R}_0$ with the corresponding contour plots. The variation in the value of $\mathscr{R}_0$ versus the effective contact rate β and quarantine rate δ is shown in Fig. 3. It is observed that $\mathscr{R}_0$ decreases for values smaller than 1 with a decrease in β and an increase in δ. Similarly, $\mathscr{R}_0$ can be reduced to a smaller value less than 1 with the increase in hospitalization/self-isolation rate γ and decrease in the effective contact rate β. This interpretation can be found in Fig. 4. The combined effect of the infectious rate due to hospitalized infected patients ψ and δ is analyzed in Fig. 5 while the behavior of $\mathscr{R}_0$ for the variation in τ and δ is depicted in Fig. 6. This interpretation demonstrates that $\mathscr{R}_0$ can be

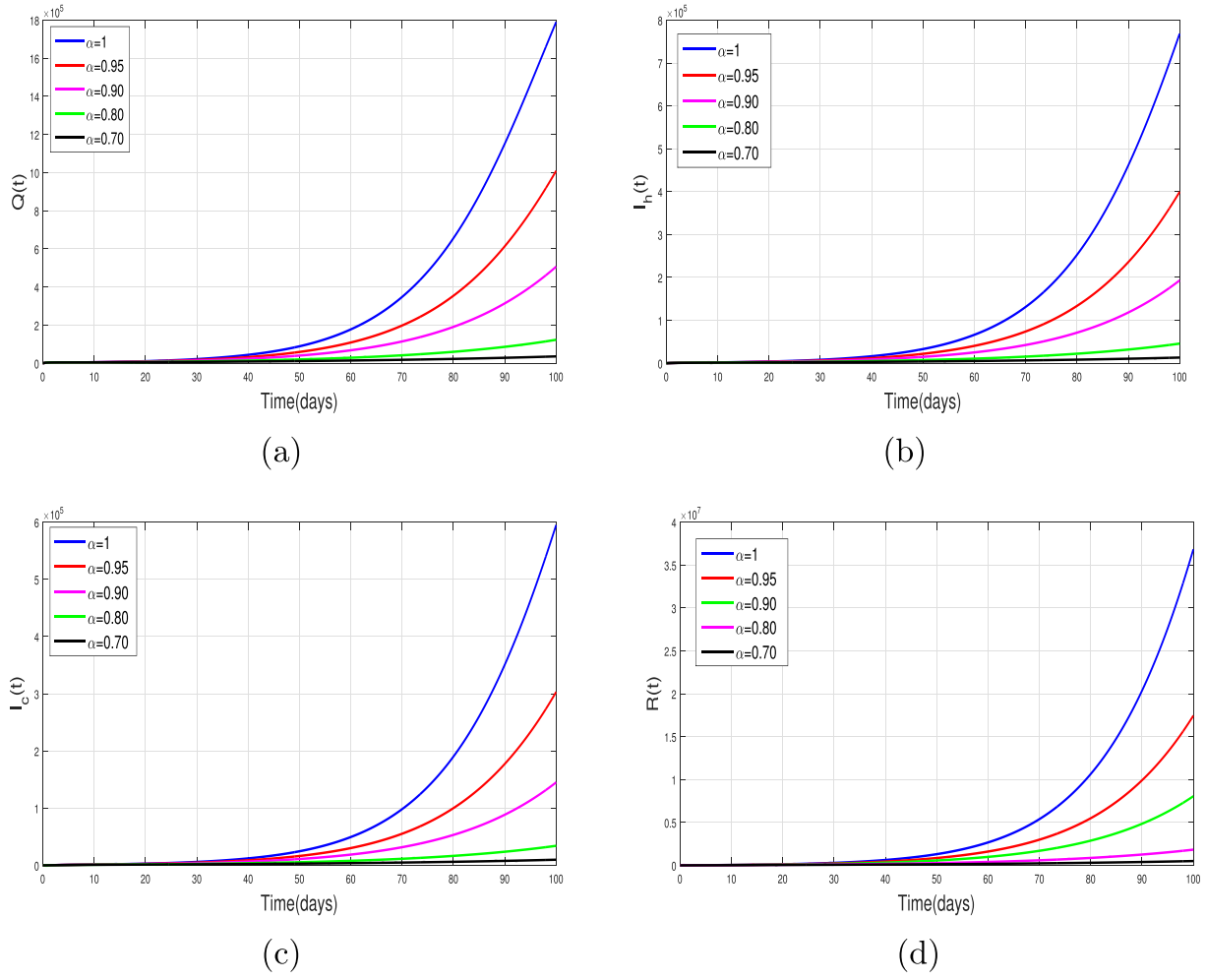

Fig. 9. Dynamics of fractional COVID-19 model for different values of α.

effectively reduced with a reduction in the effective infectious rates (τ and δ) and enhancing the efficacy of contact-tracing and quarantine policies of the exposed population. Finally, we analyzed the role of variation of both quarantine rate γ and hospitalization rate γ on the value of $\mathscr{R}_0$. It is worth mentioning that $\mathscr{R}_0$ remains very smaller with an increase in both these parameters.

6. Numerical results and discussion

This section presents the numerical results of the Caputo COVID-19 model (6). The generalized predictor–corrector of Adams–Bashforth Moulton method developed in [13,11] is considered for the numerical solution of the model (6). To simulate the model, we use the real parameters fitted given in Table (2). To study the model qualitative behavior and its parameters effect on the system and possible control, we varied the model important parameters and the fractional order α and obtained the simulation results. We studied graphically the coronavirus model (6) for five different values of α are shown in Figs. 8 and 9. It is observed that the susceptible population is increased while the population in all remaining classes is decreased significantly, when the fractional order α takes smaller values. The impact of effective contact rate β on the dynamics of symptomatic and asymptomatic infected individuals is shown in Fig. 10 for four different values of fractional order α of the Caputo derivative. A significant decrease in newly reported symptomatic and asymptomatic infected individuals is seen with a decrease in β. Further, with a 40% decrease in effective contacts (i.e., $\beta = 0.4683$) to its estimated baseline value, a dramatic decrease is observed in the peak of infection curves. This trend is observed for all values of α, but for smaller values of fractional order, the decrease in the infection curves is comparatively more significant. Fig. 11 illustrates the influence of effective contacts β on the behavior of hospitalized and critically infected (or ICU patients). It is seen that the total hospitalized and the critically infected population is decreased very well when β is decreased at 10%, 20%, 30% and 40% respectively to its baseline value as shown in Fig. 11. Moreover, the decrease in the cumulative hospitalized and critically infected individuals becomes more significant for smaller values of fractional order α. As a consequence of this graphical interpretation, the severity of COVID-19 infection can be reduced by following a strict Standard Operating Procedure (SOPs) in order to reduce the effective contacts among infected and susceptible individuals. The impact of quarantine rate or contact-tracing parameter δ on the dynamics of symptomatic and asymptomatic infected individuals is analyzed in Fig. 12. From this analysis one can observe that with an increase in δ (up to 50 % i.e. $\delta = 0.5574$) to the baseline value a sharp decrease in the peak of infected curves is seen as shown in Fig. 12. We depicted the simulations for four distinct values of α and obtained identical behavior for fractional order parameter values, that the decrease in the infected individuals is comparatively faster for smaller values of α. Furthermore, Fig. 13 depicts the dynamics of the cumulative hospitalized and critically infected population for variation in the δ. With the increase in the contact-tracing policy, a decrease in hospitalized and the critically infected population is observed. The same

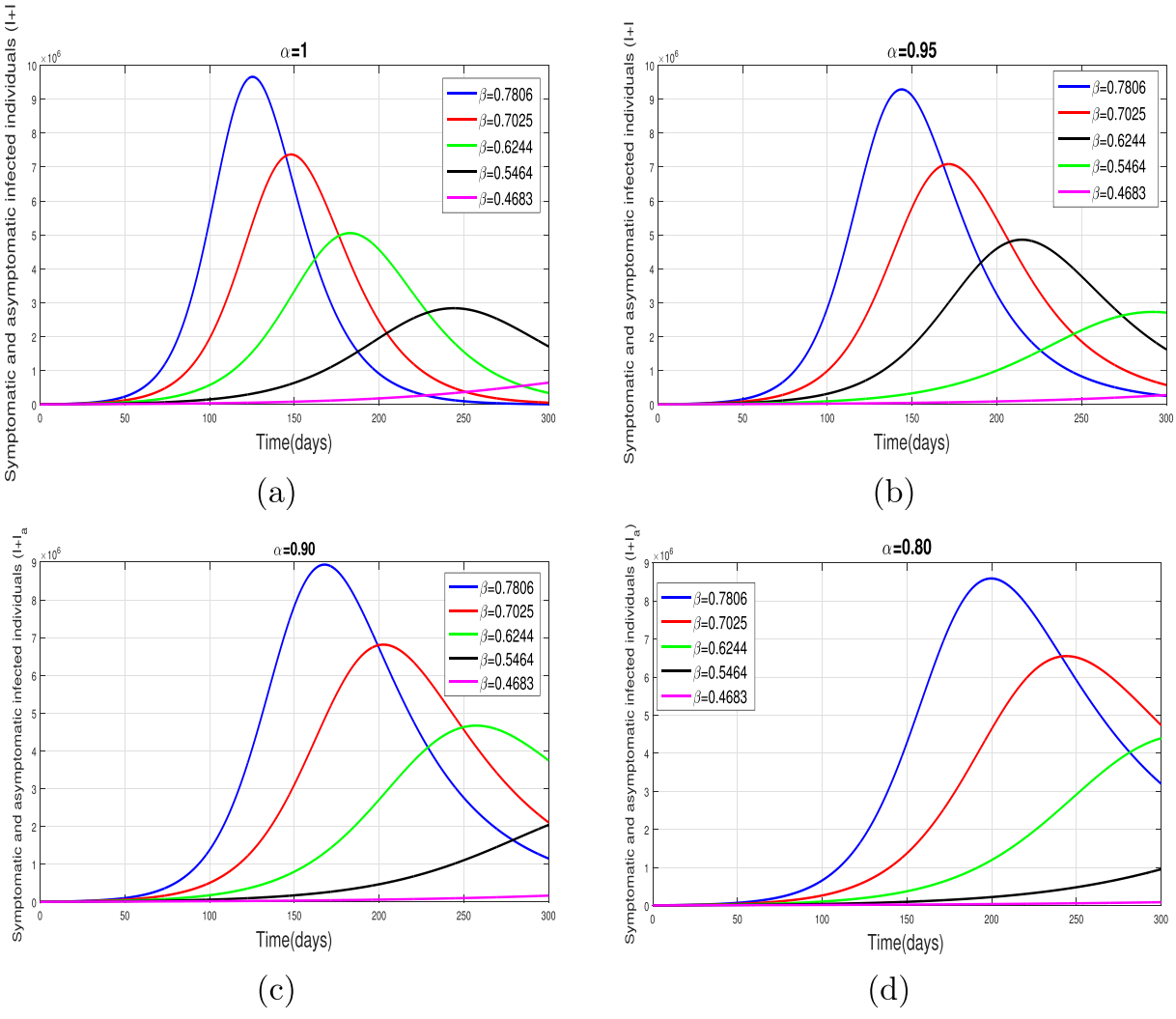

Fig. 10. Influence of δ (quarantine rate) on the symptomatic and asymptomatic infected individuals with different value of α.

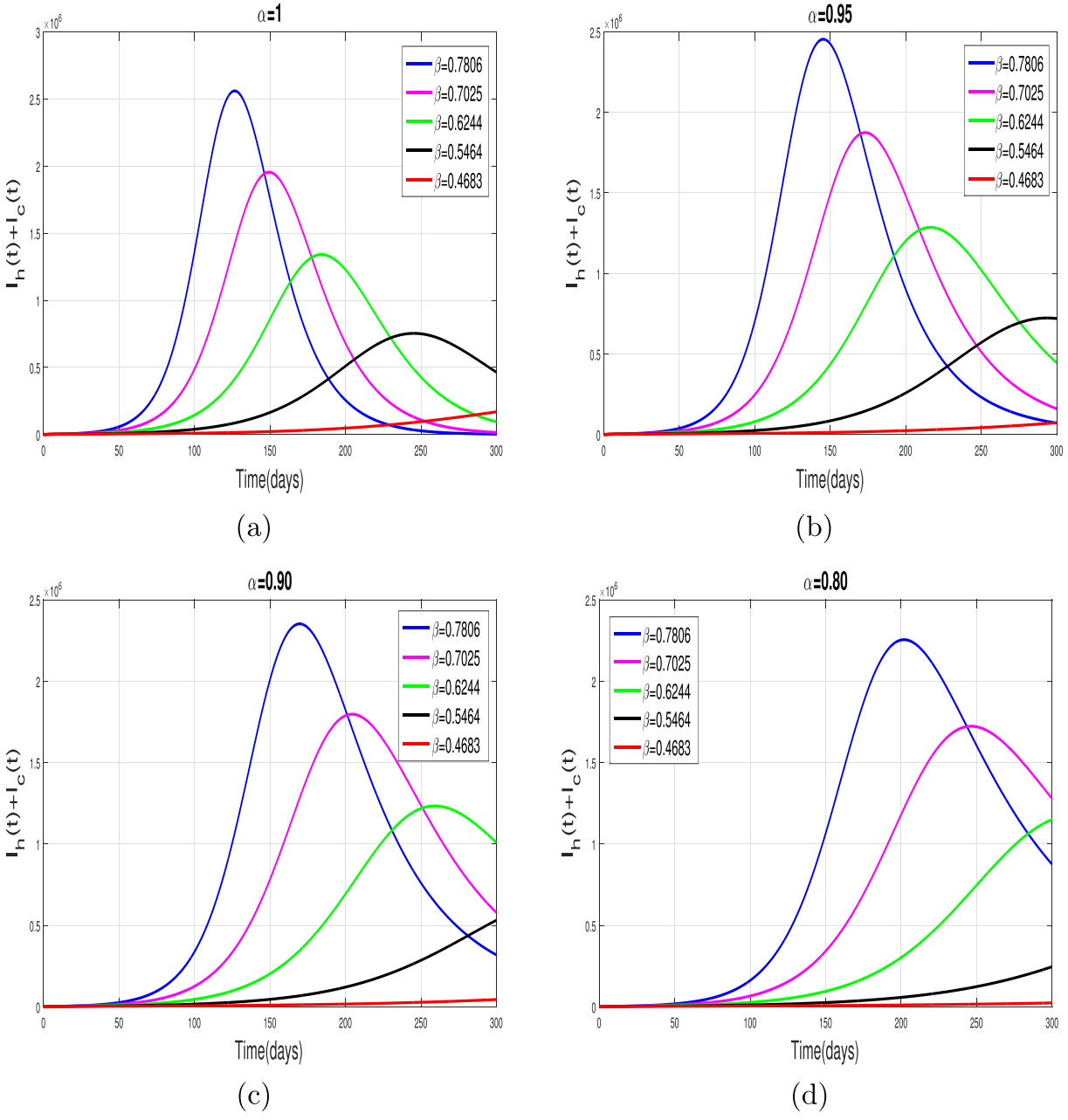

Fig. 11. Impact of β (contact rate) on the hospitalized and ICU infected individuals with different value of α.

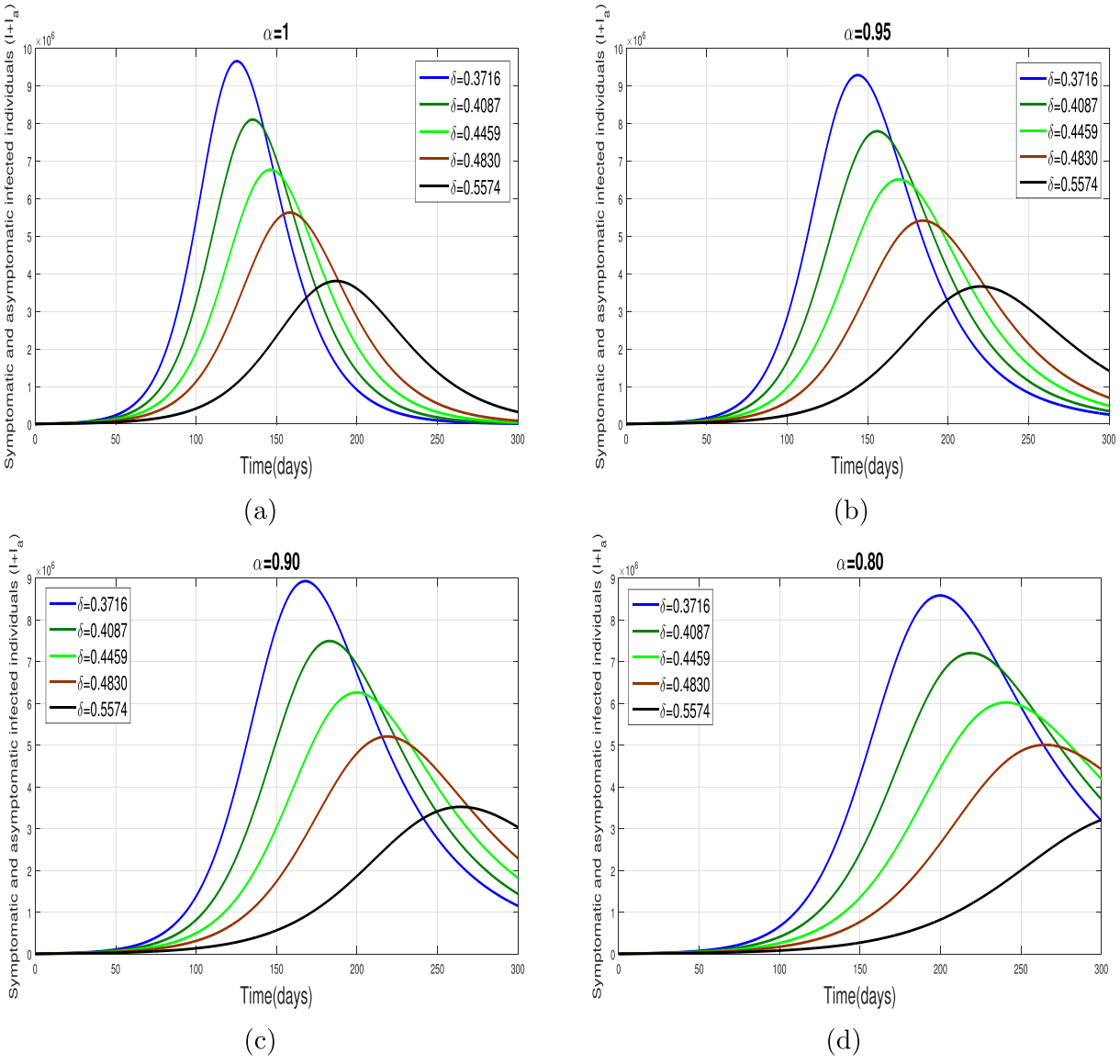

Fig. 12. Influence of δ (quarantine rate) on the symptomatic and asymptomatic infected individuals with different value of α.

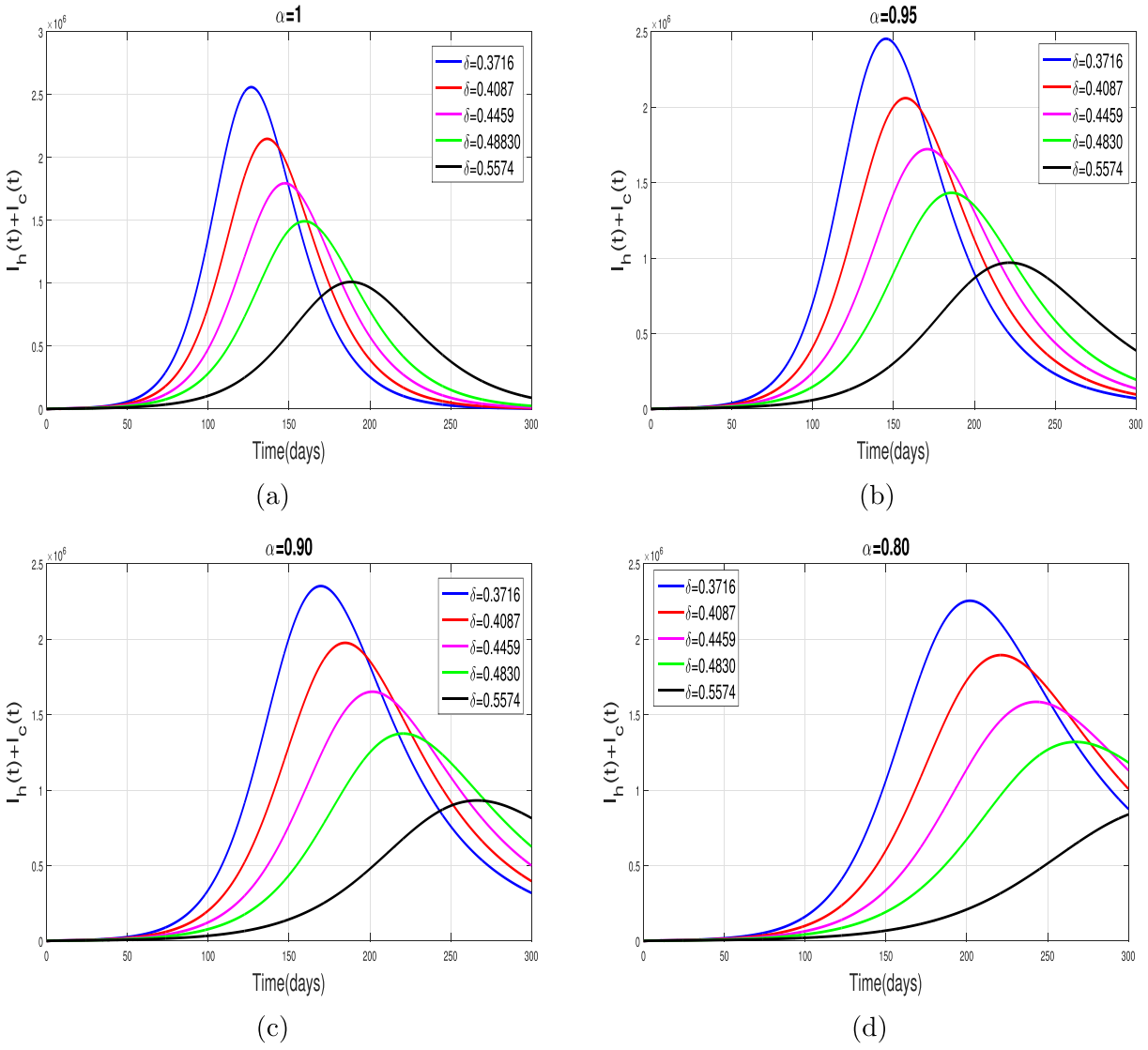

Fig. 13. Influence of δ (quarantine rate) on the hospitalized and ICU infected individuals with different value of α.

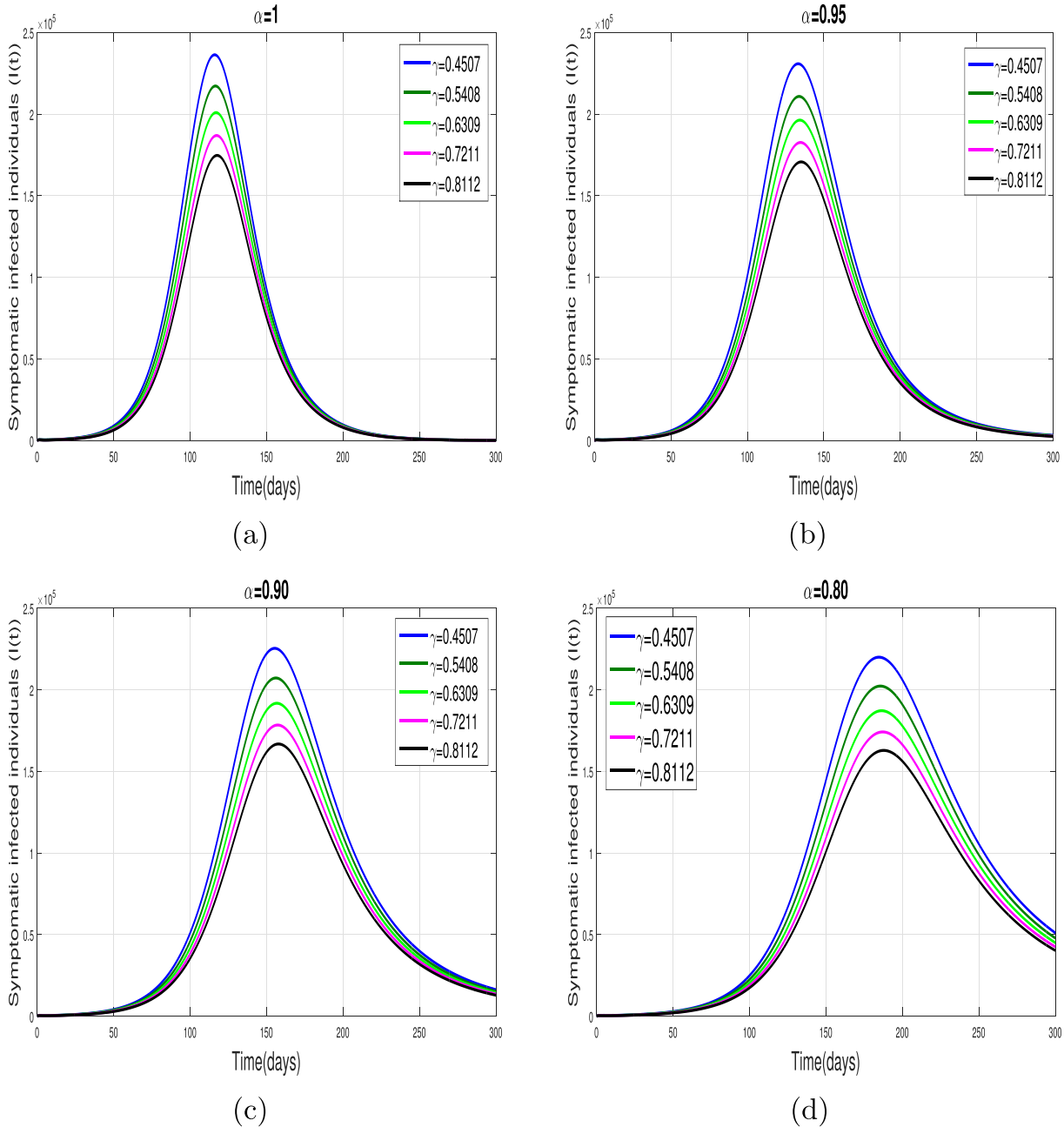

Fig. 14. Influence of γ (isolation/hospitalization rate) on symptomatic COVID-19 infected individuals with different value of α.

patterns are found for all values of fractional order α. Finally, we analyzed the influence of hospitalization of confirmed COVID-19 cases (γ) on the new cumulative symptomatic individuals. The resulting graphical interpretation for four distinct values of α is shown in Fig. 14. A small variation in the proportion of symptomatic individuals occurs even if we increase γ at a significant rate. It is found that when α decreases, the variation in the infected population is slightly feasible.

7. Conclusion

Fractional order derivatives are more prominent and provide comparatively deeper insights about real-world problems. Moreover, the derivative with fractional order is capable to capture the fading memory and crossover behavior found in most biological phenomena including infectious diseases. In this paper, we studied the dynamics of the COVID-19 outbreak in Pakistan using a fractional order mathematical model in Caputo sense which is the most commonly used operator in the modeling approach. Initially, the Caputo fractional COVID-19 model is formulated and then provided its basic and necessary mathematical properties that include the existence and positivity of the system and its solution. The detailed stability results both local and global for DFE and EE are explored using fractional stability approaches. The impact of variation in various model important parameters on the dynamics of the basic reproduction number is depicted graphically. Furthermore, the model parameters and the basic reproduction number $\mathscr{R}_0$ are estimated from the COVID-19 real infective reported cases from health ministry of Pakistan from the start of the outbreak till June 30, 2020. The non-linear least square procedure is used for the estimation purpose. The present finding showed that the results of predictions obtained through our model is inline with those published in literature and thus more appropriate values of the parameters are estimated. The numerical value of the basic reproduction number evaluated using the parameters

obtained from fitting is $\mathscr{R}_0 \approx 1.8870$ which is inline to the published result in [32]. Finally, we simulated the Caputo model in order to examine the impact of various NPIs on the dynamics and control of COVID-19 in Pakistan. We varied the relevant parameters at different levels to its baseline values and obtained the graphical results for distinct values of fractional order α of the Caputo derivative. It is found that the reduction in the effective contacts β (up to 40 %) and an enhancement in contact-tracing policy to quarantine the exposed individuals δ (up to 50%) to its baseline value that dramatically reduced the peak of infected curves. Moreover, the reduction in the infected population becomes more significant for smaller values of fractional order α. Thus we conclude that the results obtained for the fractional case are reliable, realistic and more biologically feasible. In future, the present study can be extended to fractional order with the non-singular kernel.

CRediT author statement

Fehaid Salem Alshammari: Conceptualization, Methodology, Aatif Ali: Conceptualization, Methodology, Writing- Original draft preparation, Saif Ullah: Data curation, Writing- Original draft preparation, Software, Muhammad Altaf Khan: Conceptualization, Methodology, Writing- Original draft preparation, Supervision, Reviewing and Editing, Saeed Islam: Conceptualization, Methodology, Supervision.

Declaration of Competing Interest

The authors declare that they have no known competing financial interests or personal relationships that could have appeared to influence the work reported in this paper.

References

[1] Pakistan Population 1950–2020.https://www.worldometers.info/world-population/pakistan-population, accessed 30th June 2020, 2020.
[2] Alshammari Fehaid Salem. A mathematical model to investigate the transmission of COVID-19 in the kingdom of Saudi Arabia. Comput Math Methods Med October 2020;2020:1–13.
[3] Atangana Abdon. Non validity of index law in fractional calculus: a fractional differential operator with markovian and non-markovian properties. Physica A 2018;505:688–706.
[4] Atangana Abdon. Modelling the spread of covid-19 with new fractal-fractional operators: Can the lockdown save mankind before vaccination? Chaos Solitons Fractals 2020;136:109860.
[5] Atangana Abdon, Dumitru Baleanu. New fractional derivatives with nonlocal and non-singular kernel: theory and application to heat transfer model. arXiv preprint arXiv:1602.03408; 2016.
[6] Atangana Abdon, Gómez-Aguilar JF. Decolonisation of fractional calculus rules: breaking commutativity and associativity to capture more natural phenomena. Eur Phys J Plus 2018;133(4):166.
[7] Atangana Abdon, Gómez-Aguilar JF. Fractional derivatives with no-index law property: application to chaos and statistics. Chaos Solitons Fractals 2018;114:516–35.
[8] Atangana Abdon, Koca Ilknur. Chaos in a simple nonlinear system with atangana–baleanu derivatives with fractional order. Chaos Solitons Fractals 2016;89:447–54.
[9] Baleanu Dumitru, Jajarmi Amin, Bonyah Ebenezer, Hajipour Mojtaba. New aspects of poor nutrition in the life cycle within the fractional calculus. Adv Diff Eqs 2018;2018(1):1–14.
[10] Baleanu Dumitru, Mohammadi Hakimeh, Rezapour Shahram. A fractional differential equation model for the covid-19 transmission by using the caputo–fabrizio derivative. Adv Diff Eqs 2020;2020(1):1–27.
[11] Carvalho Ana RM, Pinto Carla MA. Non-integer order analysis of the impact of diabetes and resistant strains in a model for tb infection. Commun Nonlinear Sci Numer Simul 2018;61:104–26.
[12] Center for Disease Control and Prevention (CDC).https://www.cdc.gov/coronavirus/2019-ncov/index.html; 2020.
[13] Diethelm Kai, Freed Alan D. The fracpece subroutine for the numerical solution of differential equations of fractional order. Forschung und wissenschaftliches Rechnen 1999, 1998,:57–71.
[14] Eikenberry Steffen E, Mancuso Marina, Iboi Enahoro, Phan Tin, Eikenberry Keenan, Kuang Yang, Kostelich Eric, Gumel Abba B. To mask or not to mask: Modeling the potential for face mask use by the general public to curtail the covid-19 pandemic. Infectious Disease Modell 2020.
[15] Fanelli Duccio, Piazza Francesco. Analysis and forecast of covid-19 spreading in china, Italy and France. Chaos Solitons Fractals 2020;134:109761.
[16] Neil Ferguson, Daniel Laydon, Gemma Nedjati Gilani, Natsuko Imai, Kylie Ainslie, Marc Baguelin, Sangeeta Bhatia, Adhiratha Boonyasiri, ZULMA Cucunuba Perez, Gina Cuomo-Dannenburg, et al. Report 9: Impact of non-pharmaceutical interventions (npis) to reduce covid19 mortality and healthcare demand; 2020.
[17] COVID-19 Coronavirus Pandemic in Pakistan. https://http://covid.gov.pk/. Accessed 30th June 2020; 2020.
[18] Khan Aziz, Gómez-Aguilar JF, Saeed Khan Tahir, Khan Hasib. Stability analysis and numerical solutions of fractional order hiv/aids model. Chaos Solitons Fractals 2019;122:119–28.
[19] Khan Muhammad Altaf, Atangana Abdon. Modeling the dynamics of novel coronavirus (2019-ncov) with fractional derivative. Alex Eng J 2020.
[20] Khan Muhammad Altaf, Azizah Muftiyatul, Ullah Saif, et al. A fractional model for the dynamics of competition between commercial and rural banks in indonesia. Chaos Solitons Fractals 2019;122:32–46.
[21] Khan Muhammad Altaf, Gómez-Aguilar Francisco. Tuberculosis model with relapse via fractional conformable derivative with power law. Math Methods Appl Sci 2019;42(18):7113–25.
[22] Esteban Ortiz-Ospina Max Roser, Hannah Ritchie, Joe Hasell. Coronavirus pandemic (covid-19). Our World in Data; 2020.https://ourworldindata.org/coronavirus.
[23] Morales-Delgado VF, Gómez-Aguilar JF, Saad Khaled M, Khan Muhammad Altaf, Agarwal P. Analytic solution for oxygen diffusion from capillary to tissues involving external force effects: a fractional calculus approach. Physica A 2019;523:48–65.
[24] Odibat Zaid M, Shawagfeh Nabil T. Generalized Taylor's formula. Appl Math Comput 2007;186(1):286–93.
[25] World Health Organization.https://www.who.int/emergencies/diseases/novel-coronavirus-2019. Accessed 30th June 2020; 2020.
[26] Pinto Carla MA, Carvalho Ana RM. Diabetes mellitus and tb co-existence: Clinical implications from a fractional order modelling. Appl Math Model 2019;68:219–43.
[27] Podlubny Igor. Fractional differential equations: an introduction to fractional derivatives, fractional differential equations, to methods of their solution and some of their applications. Elsevier; 1998.
[28] Saad Khaled M, Gómez-Aguilar JF, Almadiy Abdulrhman A. A fractional numerical study on a chronic hepatitis c virus infection model with immune response. Chaos Solitons Fractals 2020;139:110062.
[29] Singh Jagdev, Kumar Devendra, Baleanu Dumitru. On the analysis of fractional diabetes model with exponential law. Adv Diff Eqs 2018;2018(1):1–15.
[30] Srivastava HM, Dubey VP, Kumar R, Singh J, Kumar D, Baleanu D. An efficient computational approach for a fractional-order biological population model with carrying capacity. Chaos Solitons Fractals 2020;138:109880.
[31] Tuan Nguyen Huy, Mohammadi Hakimeh, Rezapour Shahram. A mathematical model for covid-19 transmission by using the caputo fractional derivative. Chaos Solitons Fractals 2020:110107.
[32] Ullah Saif, Khan Muhammad Altaf. Modeling the impact of non-pharmaceutical interventions on the dynamics of novel coronavirus with optimal control analysis with a case study. Chaos Solitons Fractals 2020:110075.
[33] Ullah Saif, Khan Muhammad Altaf, Farooq Muhammad. A fractional model for the dynamics of tb virus. Chaos Solitons Fractals 2018;116:63–71.
[34] Ullah Saif, Khan Muhammad Altaf, Farooq Muhammad. Modeling and analysis of the fractional hbv model with atangana-baleanu derivative. Eur Phys J Plus 2018;133(8):313.
[35] Ullah Saif, Khan Muhammad Altaf, Farooq Muhammad, Hammouch Zakia, Baleanu Dumitru. A fractional model for the dynamics of tuberculosis infection using caputo-fabrizio derivative. Discrete Continuous Dyn Syst-S 2019:975.
[36] ur Rahman Mati, Arfan Muhammad, Shah Kamal, Gómez-Aguilar JF. Investigating a nonlinear dynamical model of covid-19 disease under fuzzy caputo, random and abc fractional order derivative. Chaos Solitons Fractals 2020;140:110232.
[37] Vargas-De-León Cruz. Volterra-type lyapunov functions for fractional-order epidemic systems. Commun Nonlinear Sci Numer Simul 2015;24(1–3):75–85.
[38] Coronavirus disease (COVID-19) technical guidance World Health Organization.https://www.who.int/emergencies/diseases/novel-coronavirus-2019/technical-guidance. Accessed 30th June 2020, 2020.
[39] Jianhong Wu, Tang Biao, Bragazzi Nicola Luigi, Nah Kyeongah, McCarthy Zachary. Quantifying the role of social distancing, personal protection and case detection in mitigating covid-19 outbreak in ontario, canada. J Math Ind 2020;10(1):1–12.